Division of Structural Engineering
Lund University

Evaluation of analytical and finite element models for design of partially anchored wood-framed shear walls

Anders Lagerås

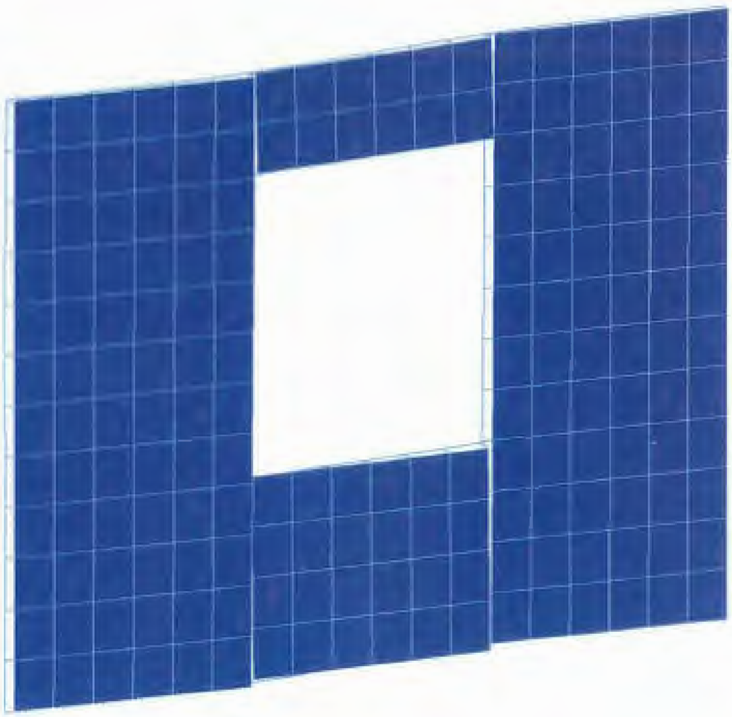

Report TVBK-5113
Lund 2002

Report TVBK - 5113
ISSN 0349 - 4969
ISRN:LUTVDG/TVBK-02/5113-SE (55 P)

Evaluation of analytical and finite element models for design of partially anchored wood-framed shear walls

Anders Lagerås

Masters Thesis

Lund University
Division of Structural Engineering
P.O. Box 118
SE-221 00
Lund Sweden

Preface

The work presented in this masters thesis has been carried out at the Division of Structural Engineering at Lund University during the autumn of 2001.

First and foremost, my thanks go to Sverker Andreasson, my supervisor, for his guidance and assistance in completing this project. I would also like to thank Bo Källsner, especially for providing results from analyses of shear walls with openings, Ulf Arne Girhammar and Liping Wu, for the experimental data, and everyone else who in one way or another contributed to this work.

Lund in January 2002

Anders Lagerås

Summary

The structural behaviour of a shear wall mainly depends on the configuration of the sheathing to framing joints, and the connections to the surrounding structure, of which the anchoring to the substrate is of major importance. However, most of the today used shear wall design methods are linear elastic models limited to the design of walls fully anchored at wall ends and openings. For the design of partially anchored shear walls none of these methods are suitable. Due to economic reasons it is, however, desirable to reduce the number of tie downs and also to predict the impact of openings accurately. Consequently, there is a need for models that are able to accurately describe the behaviour of such walls.

An analytical method, capable of dealing with partially anchored and vertically loaded walls, as well as walls with openings, has recently been developed by Källsner (Källsner et al., 2001). The model can be used in many situations. For analyses of the most complex shear wall constructions, however, more advanced methods, such as finite element models, are needed.

The main objective of this study is to compare the accuracy of the new analytical method for partially anchored and vertically loaded shear walls with the accuracy of advanced FE analyses. A further aim is to investigate the influence of different complexity concerning fastener representation on the accuracy of FE analyses.

In order to achieve these objectives, a finite element model with several possible fastener models of different complexity, have been developed in the general finite element analyses program ANSYS. The finite element model is based on a model developed by Andreasson (2000). However, some improvements of the model, mainly concerning the fastener representation, have been made. In the original model, the fastener representation was assumed to be too simplified due to the use of de-coupled springs, which implies a divergence between the direction of the fastener force and the fastener deflection. In order to make the fastener representation more realistic, beam elements with a bilinear or multi-linear isotropic material model were used to represent the fastener elements in the improved model. Results from experimental tests of hardboard sheathed shear walls and plywood sheathed shear walls were used to calibrate the model. For each fastener model, material properties for both hardboard sheathed walls and plywood sheathed walls were derived in the calibration process

After the calibration, analyses for nine different wall configurations, seven hardboard sheathed and two plywood sheathed, have been performed. Except wall geometry, the differences between the test walls include various anchorage and framing joint configurations, and different loading conditions. In order to make it possible to study the effect of sheet to sheet contact in the models, the same analyses were performed both with and without contact elements between adjacent sheets. The effect of framing and panel stiffness was also studied. All analyses have been performed with three different fastener models, i.e. beam elements with a bilinear material model, beam elements with a multi-linear material model and the original model with two de-coupled non-linear spring elements.

The results obtained from the FE analyses have been compared with experimental data, respective results obtained from the analytical method, for each wall

configuration. Mainly the load carrying capacity is evaluated since this is the only common value that can be obtained from both the analytical and the finite element model and thus be compared with experimental results. Also ratios between the experimental load carrying capacity and corresponding results obtained from the FE analyses and the analytical model, have been used to evaluate the results. Furthermore, figures showing the deformation of the framing and the position of plasticized fastener elements have been analysed in order to investigate the behaviour of the FE models and to make comparisons with the assumed force distribution in the analytical model.

The results from the analyses show that the new analytical model gives results of the same accuracy as the best finite element model used in this study. However, the change of the load carrying capacity (in respect of positive or negative change) that is almost identical between the experimental results and the most advanced FE model, is more arbitrary between the experimental results and the analytical model. The ratios between calculated and experimental load carrying capacities for the analytical method vary between 0.74 - 1.09 and corresponding ratios for the best FE model vary between 0.79 - 1.14.

The results also show that it is not possible to take full advantage of the positive effects of vertical load when using any of the methods tested. The experimental load carrying capacity is far more increased than the capacity obtained from any of the models.

Concerning the different FE models, it can be concluded that the most accurate way of modelling a shear wall with finite elements ought to be to use a realistic stiffness for framing and panel elements, and to use multi-linear beam elements as fastener elements. A bilinear fastener model implies a much less accurate fastener representation. The poor function is due the fact that these elements do not take the unloading after maximum load in the force-deflection relationship into account. Furthermore, it can be observed that the use of contact elements in order to simulate the effects of contact between adjacent sheets does not affect the behaviour of the models significantly for walls without openings. The difference is less than 1%. For a wall with opening however, the difference is about 20%.

The FE analyses also showed that the use of beam elements instead of de-coupled spring elements as fastener representation in FE models gives no major improvement of the model accuracy.

To conclude, it can be stated that the new analytical model gives results of the same accuracy as the best finite element model used in this study. The analytical model has proven to be quite accurate for analyses of different walls compared to experimental results, also for more complex wall configurations.

Table of Contents

1 Introduction

1.1 Background

The structural behaviour of a shear wall mainly depends on the configuration of the sheathing to framing joints, and the connections to the surrounding structure, of which the anchoring to the substrate is of major importance. However, most of the today used shear wall design methods are linear elastic models limited to the design of walls fully anchored at wall ends and openings. For the design of partially anchored shear walls none of these methods are suitable. Due to economic reasons it is, however, desirable to reduce the number of tie downs and also to predict the impact of openings accurately. Consequently, there is a need for models that are able to accurately describe the behaviour of such walls.

An analytical method, which is capable of dealing with partially anchored and vertically loaded walls, as well as walls with openings, has recently been developed by Källsner (Källsner et al., 2001). The model can be used in many situations, but for analyses of the most complex shear wall constructions, more advanced methods, such as finite element models, are needed.

The capacity of modern personal computers makes it possible to use rather complex models in the design work, e.g. by taking the effects of flexible joints and anchorage connections into consideration, which current analytical design models do not allow. An excellent tool for such analyses is the finite element method. FEM is a numerical technique, well suited for computers, with which help several general differential equations can be solved simultaneously. It is a very powerful tool for solving a wide variety of problems, among them structural mechanical problems, such as analyses of the structural behaviour of shear walls of all kinds. The multifaceted nature of FEM makes it a very good complement to analytical shear wall design methods.

However, it is important to limit the complexity also when using this kind of models in order to keep the time for calculation and the amount of input needed down to a reasonable level. Due to this, it is of major importance to know how different levels of model complexity affects the accuracy of the model. It is also of great interest to know the difference in accuracy between more advanced FE models and the available analytical models.

1.2 Objectives

The main objective of this study is to compare the accuracy of the new analytical method for partially anchored and vertically loaded shear walls with the accuracy of advanced FE analyses. A further aim is to investigate the influence of different complexity concerning fastener representation on the accuracy of FE analyses.

1.3 Methods

A finite element model has been developed in the general finite element analyses program ANSYS 5.7 and its script language APDL. The work is based on the scripts written by Andreasson (Andreasson, 2000). More and less complex models have been developed in order to determine the level of detail needed for an accurate solution.

The difference in complexity between the models is mainly related to the nature of the fastener elements used, in respect of type of element and material. Experimental results from tests of hardboard sheathed shear walls (Wu, Girhammar and Källsner, 2002) and plywood sheathed shear walls (Andreasson, 2000) are used to calibrate the material model for the fastener elements. Finite element analyses are then performed with each model for different anchorage, wall and loading configurations. The results of these analyses are compared to corresponding analyses performed with the analytical calculation method and with the experimental results. Quotients between the shear wall capacities obtained from the FE analyses, the analytical calculations and the experiments are used in order to evaluate the results.

1.4 Limitations

The asymmetry caused by the fact that sheathing panels may be attached to only one side of the framing is not taken into account in the finite element model. Neither is out of plane buckling of the panels or effects such as timber failure taken into account. The framing and sheathing are assumed to be homogenous and isotropic. Non-linearity is only considered for sheathing fasteners and framing joints. Further more the effects of different framing joints have not been examined, except for the case when no framing joint connections exist.

2 Analytical models

In the design of shear walls, analytical methods are normally used. Most frequently used are the linear elastic methods, but also plastic methods are available. Although a number of different variants exist, the usage of all these methods have been limited to design of fully anchored walls. However, a new analytical method that can be used for analyses of partially anchored shear walls, has been presented by Källsner (Källsner et al., 2001).

In the following, some of the available models that are currently used in practical design will be outlined, as well as the new model developed by Källsner.

2.1 Current methods

In Carling et al. (1992) three methods for design of wood framed shear walls are described. In all of these methods, the framing members are assumed to be rigid and hinged to each other, and the sheets to be rigid and not to buckle. Furthermore, the sheets are assumed to have no contact with adjacent sheets or other parts of the structure. The displacements are assumed to be small compared to the dimension of the sheets. The most important requirement that must be fulfilled in order to use these methods is that the wall must be fully anchored to the substrate.

2.1.1 Linear elastic method

In the linear elastic method, also the sheathing to framing joints are assumed to be linear elastic until failure. The maximum capacity of the wall unit is reached when the first fastener reaches its failure capacity.

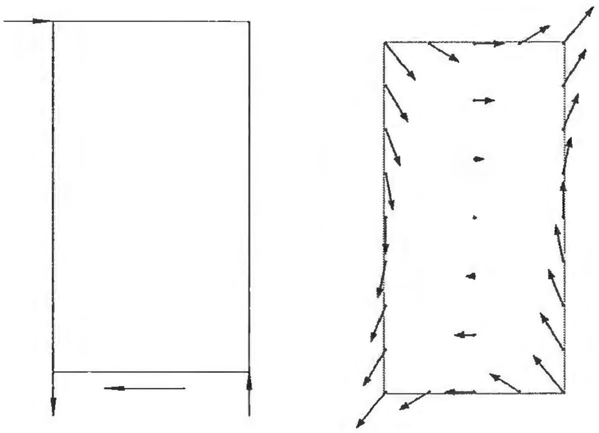

Figure 2.1: To the left, forces acting on a wall unit. To the right, force distribution on the sheet according to the linear elastic model (after Källsner et al., 2001).

The load carrying capacity of the wall unit, Figure 2.1, is determined using the linear elastic method, as described below. The load carrying capacity H_{vd} is obtained from;

$$H_{rd} = \frac{F_{vd}}{h\sqrt{\left(\frac{x_{\max}}{\sum x_i^2}\right)^2 + \left(\frac{y_{\max}}{\sum y_i^2}\right)^2}}$$

The expression is derived from rotations and a method based on finding the minimum of potential energy of one wall unit (for details see Step 3 Chapter 15). In this equation x_{max} and y_{max} are the coordinates of the fastener at the largest distance from the centre of rotation of the sheet, i.e. the fastener that carries the largest load. $\sum x_i^2$ and $\sum y_i^2$ are the sum of the coordinates for every fastener squared, h is the height of the wall and F_{vd} is the capacity of a fastener. Simplified expressions for $\sum x_i^2$ and $\sum y_i^2$ can be found in tables.

For a wall consisting of several such wall units, the load carrying capacity of the whole wall is assumed to be the sum of the load carrying capacity of each wall unit. For shear walls with openings, wall units with openings are assumed not to carry any load. The load carrying capacity of the wall is calculated by simply neglecting the units with openings and adding only the load carrying capacity of the full size wall segments. This procedure is also used for the two plastic models described below.

2.1.2 Plastic lower bound method

In the plastic lower bound method, the sheathing to framing joints are instead assumed to be completely plastic. Each sheathing fastener is assumed to carry the same load F parallel with the framing member to which it is attached, except those in the corners of the sheets, see Figure 2.2. The corner fasteners are assumed to carry F/2 in the two directions of the sides of the sheet. The fastener spacing along the edge of the sheet must be constant and the fasteners in the centre stud are assumed not to carry any load.

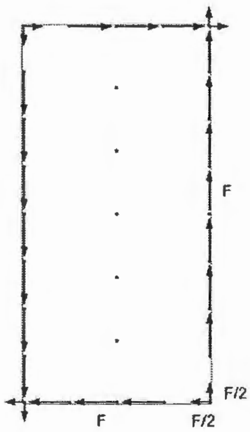

Figure 2.2: Force distribution on the sheet according to the plastic lower bound model (after Källsner et al., 2001).

Since the fasteners along the centre stud are needed to avoid buckling of the sheets, they cannot be left out in the practical design of a wall even if they are assumed not to carry any load.

2.1.3 Plastic upper bound method

In this method, the sheathing to framing joints are assumed to be completely plastic. However, in order to make the analysis a bit easier, it is possible to still use the for elastic conditions assumed centre of rotation, see Figure 2.3.

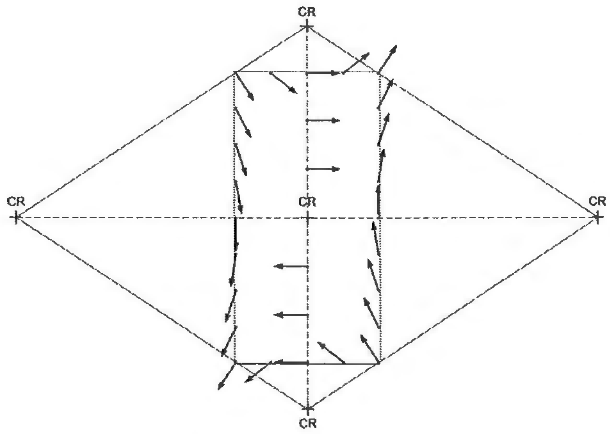

Figure 2.3: Force distribution on a sheet according to the upper bound model (after Källsner et al., 2001).

The practical use of these models is somewhat limited, since a wall with openings is treated like several separate wall segments, as described earlier. Each one of these wall segments must be fully anchored if the wall shall fulfil the requirements of the models. Furthermore, the influence of contact between adjacent sheets is neglected. In order to overcome these limitations, efforts have been made to develop new models, able to deal with partially anchored shear walls with openings.

2.2 New method

In Källsner et al. (2001) a new plastic analytical calculation method is described. The method is a plastic lower bound method capable of dealing with non anchored or partially anchored shear walls with openings and vertical load. When using this method the framing members and sheathing panels are assumed to be rigid. Furthermore, the panels are assumed not to buckle. Other assumptions made are that compressive forces can be transferred between adjacent sheets, and that displacements are small compared to the dimensions of the sheets.

Furthermore, sheathing to framing joints along the vertical studs and top rail can only transfer shear forces parallel to the frame members, while those along the bottom rail can transfer forces either parallel or perpendicular to the bottom rail. It is assumed that fasteners are completely plastic and the spacing between them is constant. It is also assumed that those attached to the centre stud do not to carry any load, except in the case of vertical load on, or anchorage of, the centre stud.

In the case of no anchoring, the hold-down force needed to prevent rotation of the wall can be provided either by a vertical force (e.g. dead load of building components), by the bottom rail fasteners or a combination of the two. The last two alternatives, of course, presupposes that the bottom rail is fixed to the substrate.

2.2.1 Fully anchored bottom rail and no vertical load

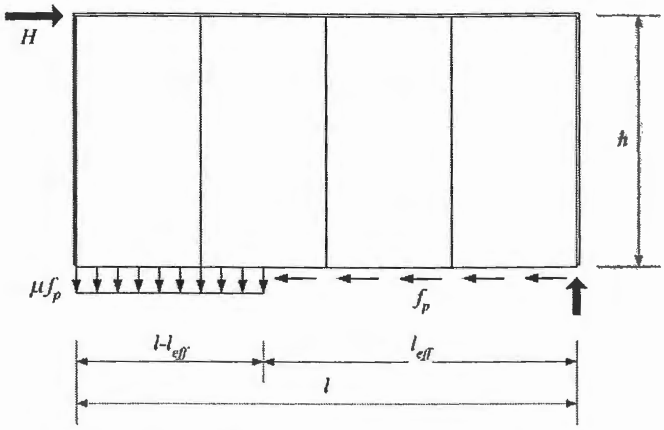

Figure 2.4: Forces acting on a shear wall with fully anchored bottom rail and no vertical load (after Källsner et al., 2001).

The bottom rail fasteners are assumed to carry load either parallel or perpendicular to the rail. Along the distance l_{eff} they carry horizontal load only and along ($l-l_{eff}$) vertical load only. The length of l_{eff} is determined by the equilibrium.

In the case of loading and anchorage as shown in Figure 2.4, the anchorage force is determined by equilibrium equations as described below.

Horizontal force equilibrium gives:

$$H = f_p \cdot l_{eff}$$

where f_p is the plastic fastener capacity per length unit.

Moment equilibrium around the lower right corner gives:

$$H \cdot h = \mu \cdot f_p (l - l_{eff}) \left(\frac{l + l_{eff}}{2} \right)$$

where μ is a reduction factor, reducing the strength of the fasteners in case of different capacity parallel and perpendicular to the panel edge.

A combination of the equations two above gives l_{eff}

$$l_{eff} = l \left(\sqrt{1 + \left(\frac{1}{\alpha\mu} \right)^2} - \frac{1}{\alpha\mu} \right)$$

where $\alpha = \dfrac{l}{h}$

The anchorage force is obtained from:

$$F_a = \mu \cdot f_p (l - l_{eff})$$

2.2.2 Fully anchored bottom rail and vertical load acting on the leading stud

In the case of vertical loading, e.g. a concentrated load at the wall end, corresponding equilibrium equations can be derived in order to calculate the wall capacity.

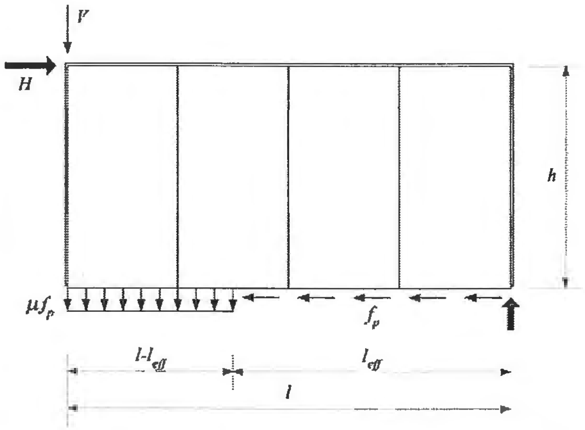

Figure 2.5: Forces acting on a shear wall with fully anchored bottom rail and a vertical load on the leading stud (after Källsner et al., 2001).

The anchorage force of the wall in Figure 2.5 is calculated as shown below.

$$\beta = \frac{V}{f_p \cdot h}$$

V is used to express the vertical load, β=1 for a wall with fully anchored leading stud.

Horizontal force equilibrium gives:

$$H = f_p \cdot l_{eff}$$

Moment equilibrium around the lower right corner gives:

$$H \cdot h - V \cdot l = \mu \cdot f_p (l - l_{eff}) \left(\frac{l + l_{eff}}{2} \right)$$

where μ is a reduction factor, reducing the strength of the fasteners.

A combination of the equations two above gives l_{eff}

$$l_{eff} = l \left(\sqrt{1 + \left(\frac{1}{\alpha\mu} \right)^2 + \frac{2\beta}{\alpha\mu}} - \frac{1}{\alpha\mu} \right)$$

where $\alpha = \dfrac{l}{h}$

The anchorage force is obtained from:

$$F_a = \mu \cdot f_p (l - l_{eff})$$

This new method represents a huge leap forward in shear wall design methods. The model makes it possible to design also partially anchored walls and to make use of vertical loads, something that is not possible when using any of the earlier described methods. However, it is not very easy to use this method for analyses of more complex wall designs and load configurations. To make it more attractive for practical use, some design tools are needed, e.g. in the form of tables or diagrams simplifying the design of common wall constructions and common load cases.

Even though this method will be very useful in many situations, it will not be possible to use it for the most complex wall designs and load cases. Since it is limited to the design of static load cases in ultimate limit state and the sheathing fasteners must show plastic behaviour, it can not be used to determine deformations. In such case the use of FE models is a better approach.

The new analytical method has so far been verified against experimental tests only for a small number of wall configurations and loading conditions. It is, thus, of major interest to further investigate the accuracy of the model. It is also interesting to compare the accuracy of the model with the accuracy of advanced finite element models.

3 Finite element model

3.1 General

The finite element model is based on the model developed by Andreasson (2000) in the general finite element program ANSYS v5.4. It is a nonlinear elastic model in 3D-space with beam, shell, spring and contact elements. In order to make the model practical to use for analyses of walls with different configurations, the pre and post processing are done with interactive scripts written in ANSYS Parametric Design Language (APDL). The model can be used to analyse a variety of shear wall configurations, e.g. with or without openings, with panels on one or both sides of the framing, with different hold-down and load configurations.

The fastener representation in the original model was assumed to be too simplified due to the use of de-coupled springs, which implies a divergence between the direction of the fastener force and the fastener deflection. In order to make the fastener representation more realistic, i.e. to have the same deflection and force direction, some improvements of the model have been made. The improvements mainly concern the fastener model, but also the modelling of sheet to sheet contact. The new adjusted model was developed in ANSYS version 5.7.

3.2 Modelling of components

The model is elastic-plastic non-linear with linear isotropic material properties for framing and panel elements, and a multi-linear isotropic material model for the fastener elements. A wall model is build up much like a physical shear wall with framing (Figure 3.1), panels (Figure 3.3), and various fasteners (Figure 3.4) that connect panels to the framing and the different framing members to each other. Effects such as contact between adjacent panels are also simulated.

3.2.1 Framing

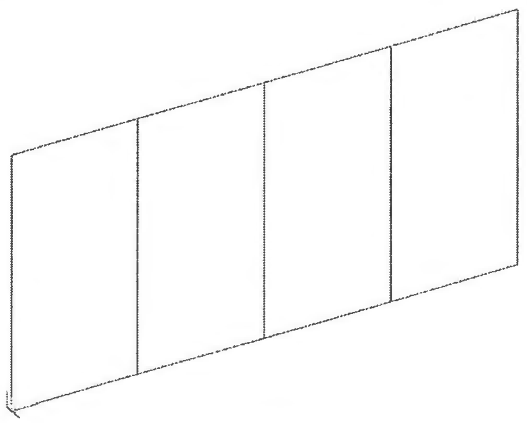

Figure 3.1: Framing built up by beam elements.

The framing members are represented with beam elements (BEAM4) with an isotropic linear elastic material model. BEAM4 is a two node, six degrees of freedom uniaxial element with tension, compression, torsion, and bending capabilities.

Since there are panels only on one side of the framing and they are attached to the framing at a certain distance (the length of the fastener elements) the model is asymmetric. In order to avoid torsion of the framing members the in plane torsional degrees of freedom parallel to the framing member have been constrained.

3.2.2 Framing joints

Three spring elements, COMBIN14 (one in X, one in Y and one in Z direction) and one contact element, CONTAC52, are used to represent the framing joints. The contact element prevents the stud elements from passing through the top and bottom rail elements but still allows uplift and sliding to occur. COMBIN14 is a two node, three degrees of freedom spring-damper element, which has longitudinal or torsional capability. CONTAC52 is a two node, three degrees of freedom node to node contact element.

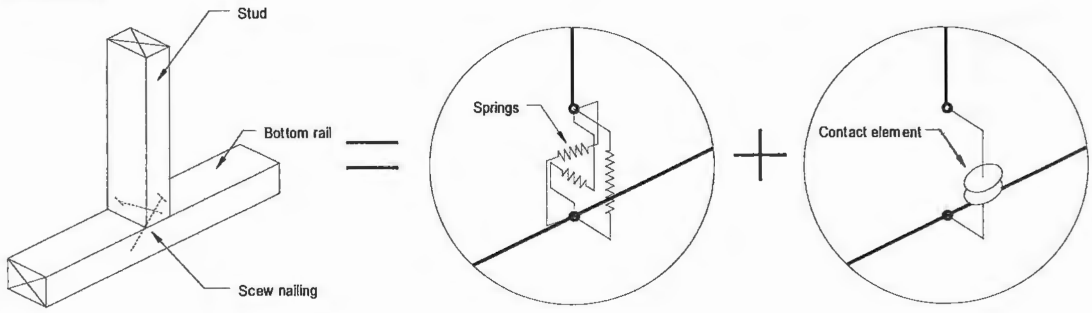

Figure 3.2: The three spring elements and the contact element representing a framing joint.

Analyses without framing joints (no springs, contact element only) and with hinged framing joints have also been performed.

3.2.3 Panels

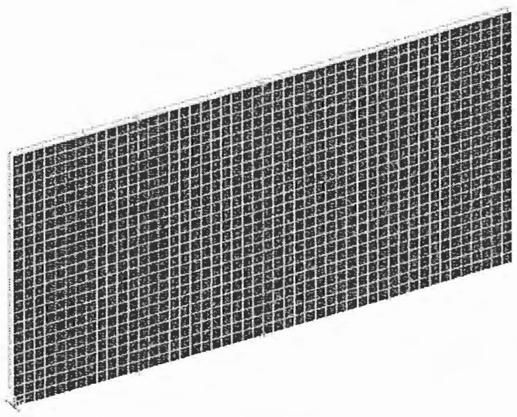

Figure 3.3: Sheathing built up by shell elements.

The elements used to represent the panels in the model are shell elements (SHELL63) with an isotropic and linear elastic material model. SHELL63 is a four node, six degrees of freedom element which has both bending and membrane capabilities. The element does not buckle in the way it is used in this model. The size of the panel element depends on the fastener spacing used. The length and height of the element is equivalent to the distance between fasteners.

3.2.4 Fasteners

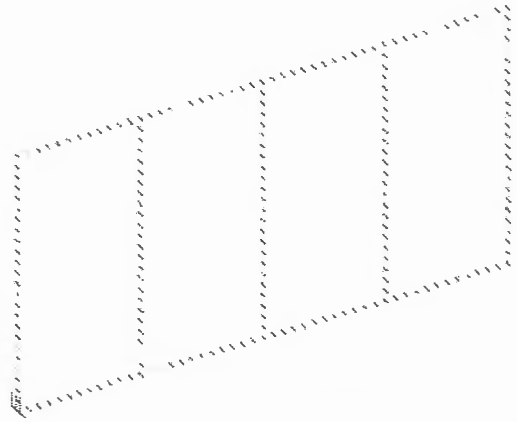

Figure 3.4: Fasteners connecting sheathing to framing.

Two different elements have been used to represent the sheathing fasteners (panel to framing joints). One is a beam element (BEAM188) with an isotropic and multi-linear plastic material model. The other element is the non-linear elastic spring element (COMBIN39) used in the model developed by Andreasson (2000).

BEAM188 is a three-node (of which one is a direction node), six degrees of freedom element, suitable for analyzing slender to moderately stubby/thick beam structures. This element is based on Timoshenko beam theory and shear deformation effects are included. BEAM188 can be used with a variety of cross sections, but for this model a circular solid cross section was chosen.

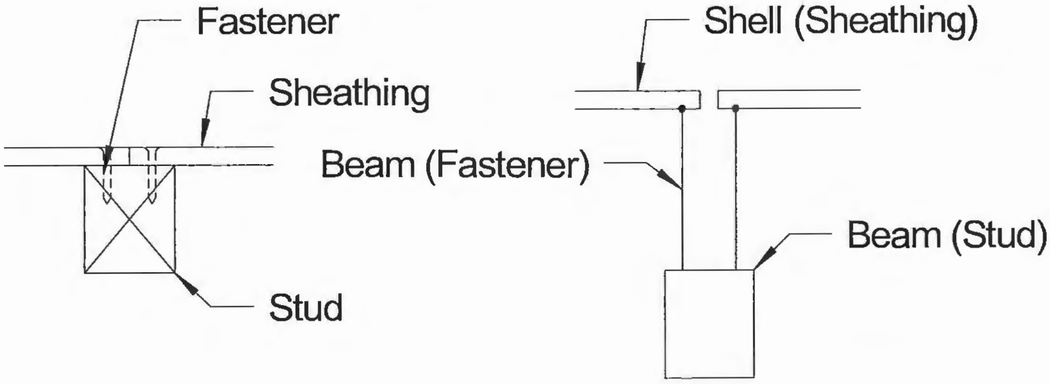

Figure 3.5: Sheathing fasteners in a shear wall to the right, and how they are represented in the FE model to the left.

In the connection between the framing and the fastener elements, the torsional and translational degrees of freedom are coupled, while only the translational degrees of freedom are coupled in the connection between the sheathing and fastener elements, as shown in Figure 3.5.

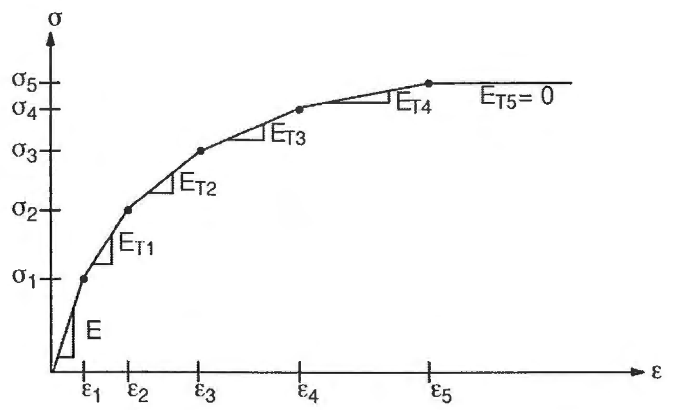

Figure 3.6: Multi-linear material behaviour (from ANSYS Theory Reference).

One of the material models used is a plastic material model called MKIN (multi-linear kinematic hardening plasticity, Figure 3.6) that use the Besseling model to characterise the material behaviour. The material is assumed to be composed by a number of sub-volumes, all subject to the same total strain, but each having different yield strength. The sub-volumes have a simple stress strain response, but when combined the model can represent complex behaviour. This allows a multi-linear stress strain curve.

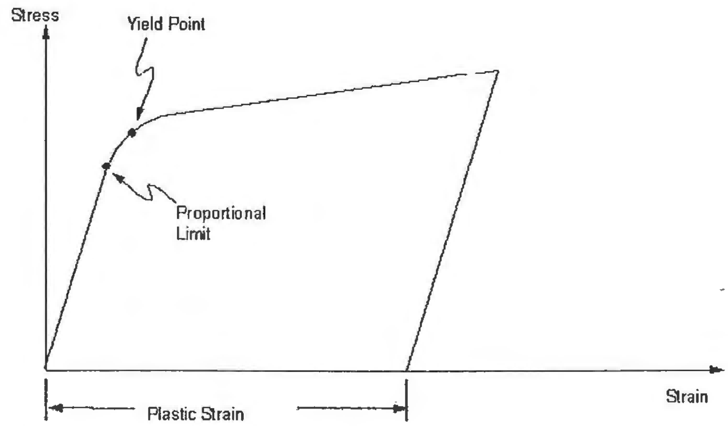

Figure 3.7: Bilinear material behaviour (from ANSYS Theory Reference).

Analyses were also performed using the model called BKIN (bilinear kinematic hardening plasticity Figure 3.7), which uses von Mises yield criterion with the associated flow rule. The use of a tangent modulus of 0 is it assumed to make the material almost ideal elastic plastic.

COMBIN39 is an unidirectional, two node, three degree of freedom spring element with nonlinear generalized force deflection capability. In order to represent the sheathing fasteners, two such de-coupled elements were used, one in horizontal and one in vertical direction. For further details, see Andreasson (2000).

3.2.5 Contact between adjacent panels

In order to make it possible for compressive forces to be transferred between adjacent sheets, contact elements (CONTAC48) are used. CONTAC48 (Figure 3.8), is a three node, two degrees of freedom point to surface contact element. Two nodes, target nodes, define a target surface which the third node, the contact node, is prevented to penetrate.

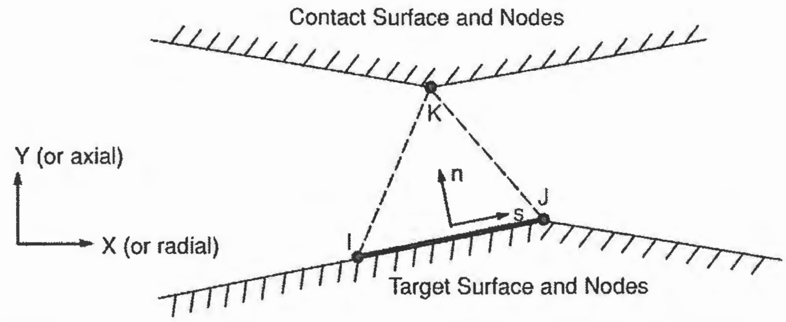

Figure 3.8: Explanatory sketch over element CONTAC48 (from ANSYS Theory Reference).

For the contact between two sheets, four contact elements are used to transfer forces in both directions, left and right, as shown in Figure 3.9.

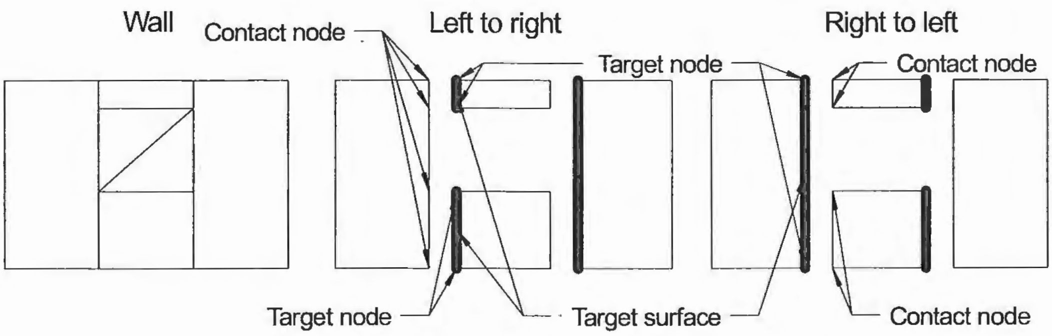

Figure 3.9: Contact elements allowing forces to be transferred between adjacent panels. The two pictures represent the same panel.

3.2.6 Boundary conditions and loading

The foundation used for the analyses of partially anchored walls consists of contact elements (CONTAC52) with all degrees of freedom for the node representing the target surface constrained to zero, see Figure 3.10.

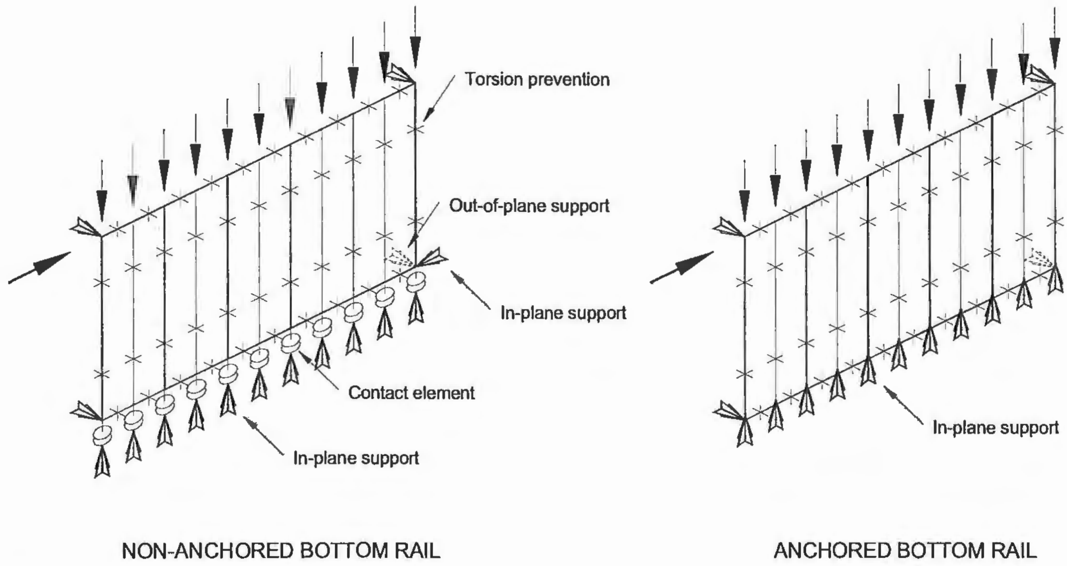

Figure 3.10: Boundary conditions for walls with non-anchored respective anchored bottom rail.

Compressive forces will be transferred to the foundation while tensile forces will not. Vertical loads are represented by forces applied to top rail nodes. The horizontal load is represented by horizontal displacement of the most left top rail nodes. A displacement controlled loading is used in order to obtain the total force-deflection curve for the wall. The horizontal degree of freedom of the right most bottom rail node is constrained. In the case of fully anchored leading stud, constraints are applied at some additional nodes.

4 FE analyses

4.1 General

In order to be able to compare the behaviour of FE analyses with experimental results and analytical calculation methods, the FE models described in chapter 3 have been used to perform several analyses for hardboard respective plywood sheathed walls. The tests of hardboard sheathed walls, test wall 1-7, are described in Källsner et al. (2001) and Wu, Girhammar and Källsner (2002), and the plywood sheathed walls, test wall 8-9, are described in Andreasson (2000), in which they are referred to as test wall B and F.

Different fastener models have been used and parameter studies have been performed concerning framing stiffness and framing joint configurations. The different FE models used are summarized in Table 4.1.

Table 4.1: Summary of models used and associated abbreviations.

Abbreviation	Explanation
Test	Experimental data
Hc	Load carrying capacity obtained with analytical calculation method
BLUS	Bilinear material model, rigid framing and panels
MLUS	Multi-linear material model, rigid framing and panels
BLLS	Bilinear material model, flexible framing and panels
MLLS	Multi-linear material model, flexible framing and panels
Nc	No contact elements between adjacent panels
SLS	Spring model, flexible framing and panel stiffness

4.2 Material properties and wall configurations

The material parameters used are collected from Andreasson (2000), and material data received from Masonite AB.

4.2.1 Hardboard sheathed walls

The hardboard sheathed walls analysed are those called test wall 1-7 in Källsner et al. (2001).

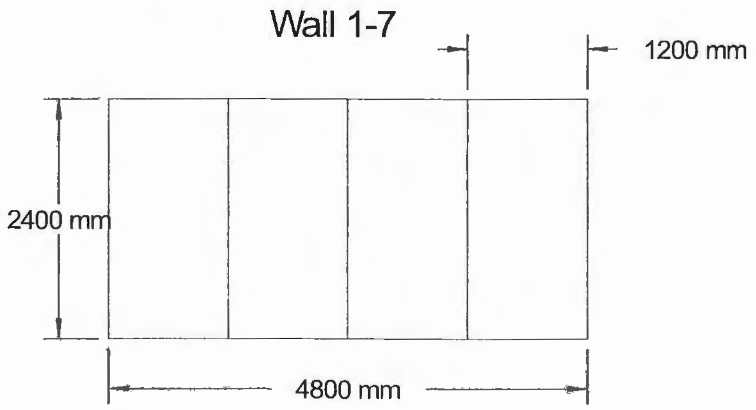

Figure 4.1: Test wall 1-7.

Each wall consists of four 1200x2400 mm panels on one side of the framing, see Figure 4.1. This makes the total length of the wall 4800 mm and the height 2400 mm. The cross section of the framing elements used is 45x120 mm and the thickness of the panels is 8 mm. The spacing of the fastener elements is 100 mm.

The material parameters used in the FE models are given in the Table 4.2.

Table 4.2: Material parameters.

Component	Property	Value	Designation
Framing	Young's modulus	10 GPa	E
Framing	Poisson's ratio	0.25	ν
Panel	Young's modulus	4.8 GPa	E
Panel	Poisson's ratio	0.412	ν

The element properties used are given in Table 4.3.

Table 4.3: Element properties

Component	Property	Value
Framing joint contact element	Normal stiffness	33 MN/m
Framing joint spring element	Spring stiffness	500 kN/m
Adjacent panel contact elements	Normal stiffness	6.7 GN/m
Foundation contact elements	Normal stiffness	68 MN/m

The spring stiffness used for the framing joint spring elements is taken from Andreasson (2000). The dimension of the fastener element (cylindrical with a radius of 1.55 mm and a length of 68 mm) when using BEAM188 element is chosen to make the element slender enough to be represented with BEAM188. The normal stiffness of the contact elements is based on the contact material stiffness and the size of the contact area.

Analyses using rigid framing and panels were also performed in order to observe the effect of framing and panel material properties on the model behaviour.

4.2.2 Plywood sheathed walls

The plywood sheathed walls analysed are those called wall B and wall F in Andreasson (2000).

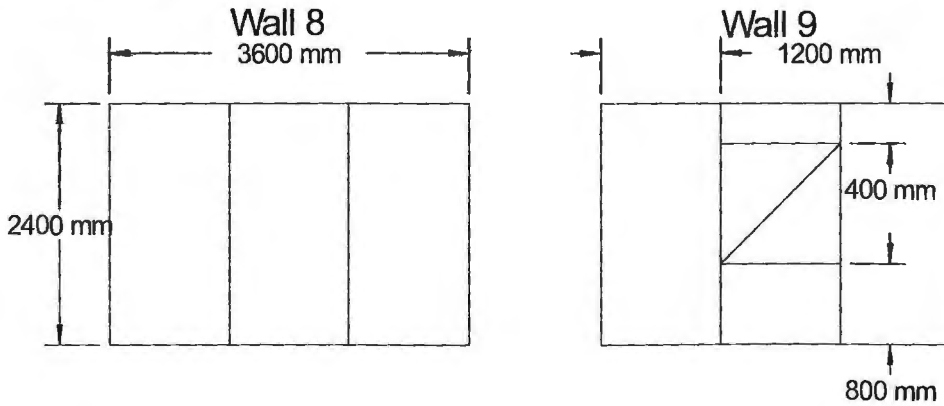

Figure 4.2: Test wall 8 and 9.

Each wall, Figure 4.2, consists of three 1200x2400 mm panels on one side of the framing. This makes the total length of the wall 3600 mm and the height 2400 mm. The panels above and below the opening in test wall 9 are 1200x400 mm and 1200 x 800 mm respectively. The cross section of the framing elements used is 45x90 mm and the thickness of the panels is 9 mm. The spacing of the fastener elements is 200 mm along the perimeter and 400 mm along the centre studs.

The material parameters used in the FE models are given in Table 4.4.

Table 4.4: Material parameters.

Component	Property	Value	Designation
Framing	Young's modulus	10 GPa	E
Framing	Poisson's ratio	0.25	ν
Panel	Young's modulus	6 GPa	E
Panel	Poisson's ratio	0.418	ν

The element properties used are given in Table 4.5.

Table 4.5: Element properties.

Component	Property	Value
Framing joint contact element	Normal stiffness	33.1 MN/m
Framing joint spring element	Spring stiffness	500 kN/m
Panel contact elements	Normal stiffness	500 MN/m
Foundation contact elements	Normal stiffness	36.6 MN/m

The spring stiffness used for the framing joint spring elements is taken from Andreasson (2000). The dimension of the fastener element (cylindrical with a radius of 1.7 mm and a length of 54 mm) is chosen to make the element slender enough to be represented with the BEAM188 element. The normal stiffness of the contact elements is based on the contact material stiffness and the size of the contact area.

4.3 Calibration of FE model

4.3.1 Fasteners for hardboard sheathed walls

The test wall 1 configuration was used to calibrate the fastener element material model against experimental data. For test wall 1 described in Källsner et al (2001), the load was applied in a diagonal direction, according to Figure 4.3, in order to obtain a pure shear action in the wall.

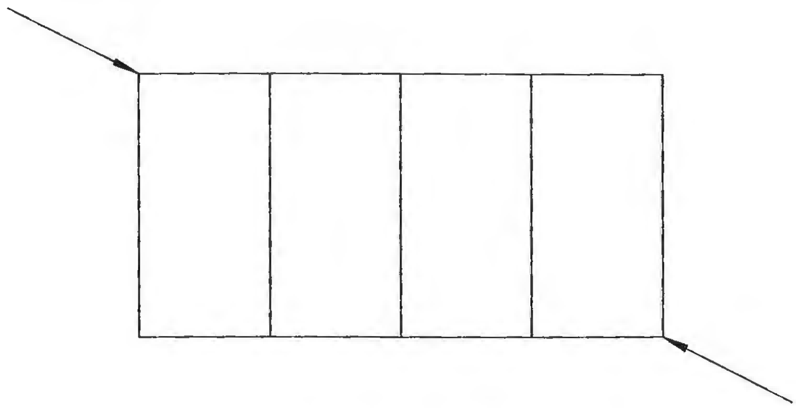

Figure 4.3: Loading and wall configuration for test wall 1.

For the calibration of the FE model the load was, however, represented by constraints of the horizontal degree of freedom of the node in the upper left corner of the framing. In order to compensate for the missing vertical load, the framing joints were hinged and the leading stud fully anchored to the foundation, see Figure 4.4.

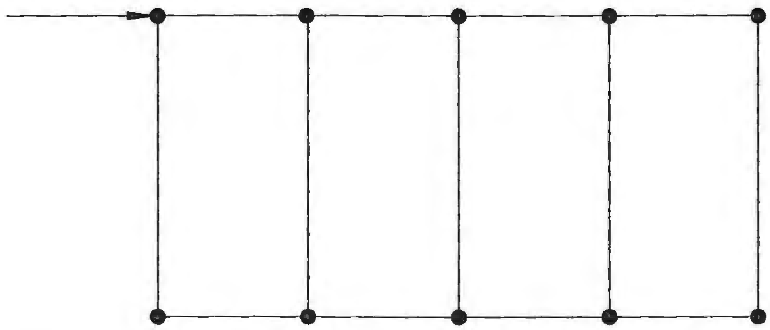

Figure 4.4: Loading and wall configuration for test wall 1 FE model.

The fastener material model was adjusted in such a way that the overall force-deflection behaviour of the FE model of the wall corresponded to the experimental force-deflection curve. The calibration of the model was performed using rigid framing and panel elements since the analytical calculation model presupposes rigidity of these components. Two different material models for use with the beam fastener element, one bilinear and one multi-linear, were calibrated. The properties of the spring element used for the third fastener model was calibrated in the same manner.

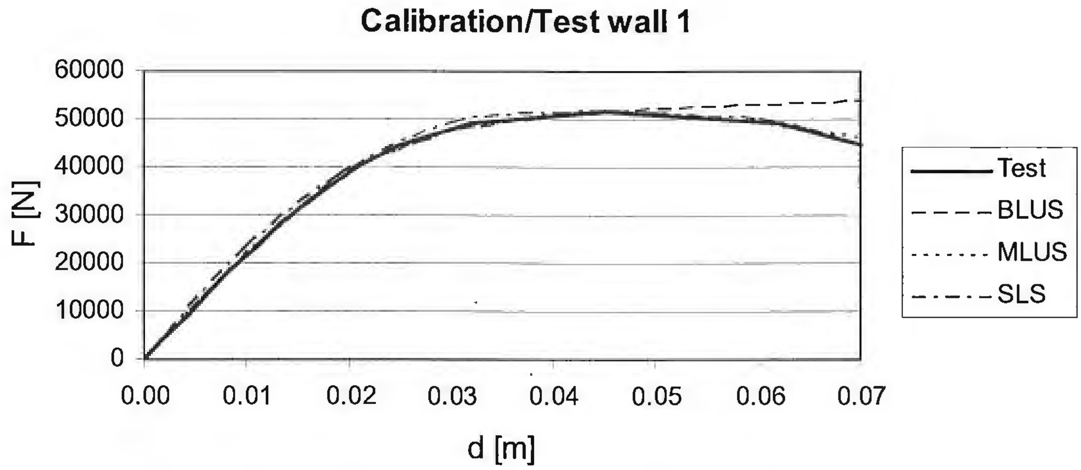

Figure 4.5: Force-displacement relationship of test wall 1 and calibrated FE models.

The force displacement relationship of the wall, see Figure 4.5, at deformations larger than 70 mm is not very well described by the experimental data used, which makes it hard to know exactly how well the force-displacement relationship of the models and the test wall agree at larger deformations.

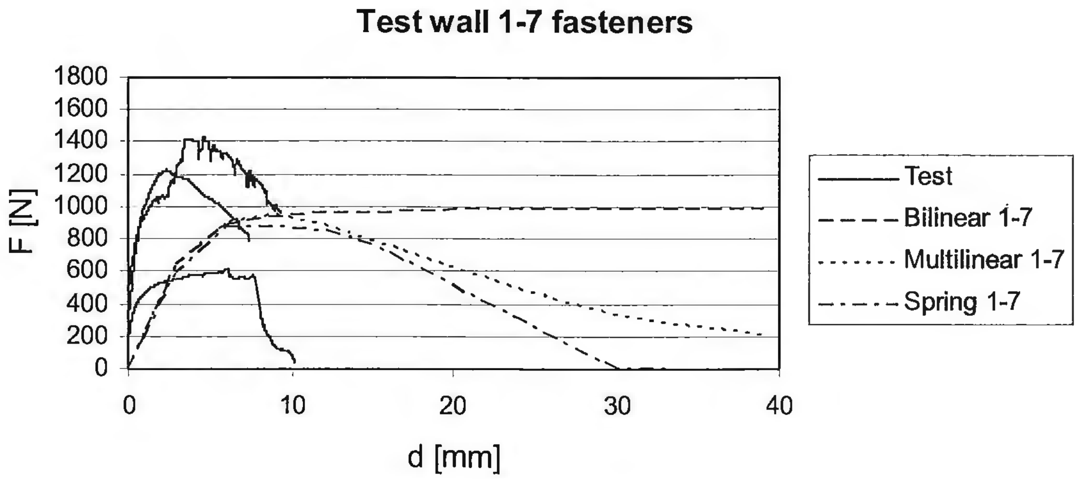

Figure 4.6: Force-displacement relationship of fasteners in tests and FE models.

As shown in Figure 4.6, the capacity of the modelled fasteners is between the lowest and highest of the capacities obtained from the three fastener tests. It can be noted that the fastener in the FE models has to be less stiff than the fasteners used in the tests in order for the modelled wall to obtain a stiffness similar to that of a full scale test wall. A possible cause is initial framing joint gaps, something that is not taken into account in the FE model.

4.3.2 Fasteners for plywood sheathed walls

Test wall 8 was used for the calibration of the fastener models used for the plywood sheathed walls. Test wall 8 is fully anchored to substrate and has vertical loads of 2.25 kN applied at the top rail at each stud, see Figure 4.7.

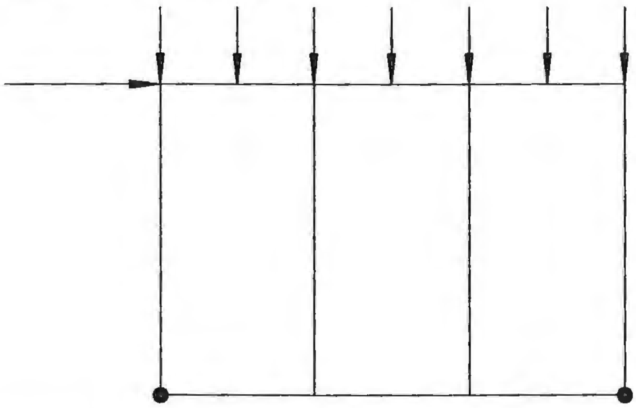

Figure 4.7: Loading and wall configuration for test wall 8.

The fastener material model was adjusted in such a way that the overall force-deflection behaviour of the FE model of the wall corresponded to the experimental force-deflection curve. The calibration of the model was performed using flexible framing and panel. Two different material models for use with the beam fastener element, one bilinear and one multi-linear, were calibrated. The properties of the spring elements used for the third fastener model was calibrated in the same manner.

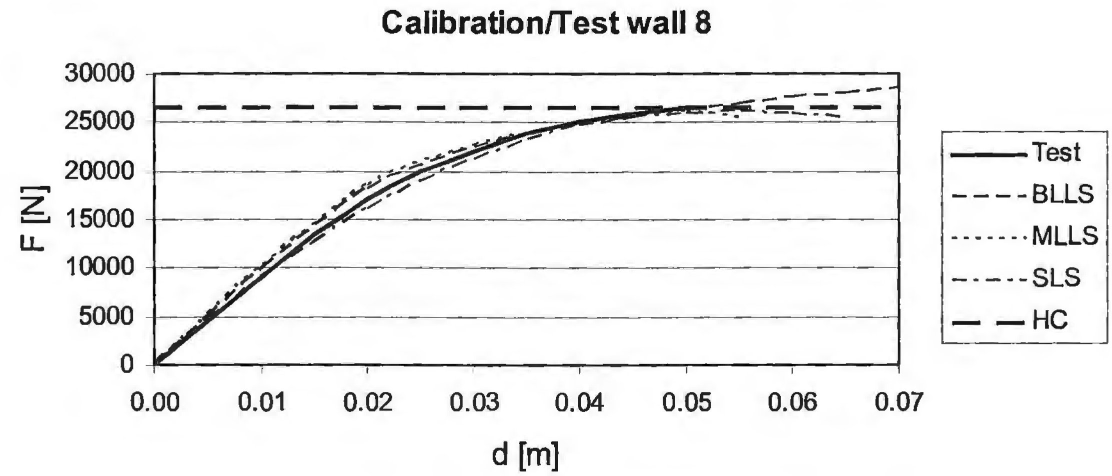

Figure 4.8: Force-displacement relationship of test wall 8 and calibrated FE models.

For larger horizontal displacement than 50 mm, for which no more test data are available, is it possible to make the capacity of the FE model to decrease when using the multi-linear fastener material model. See Figure 4.8. This, probably, corresponds more to the real behaviour, than using the bilinear material model, for which the capacity continues to increase after 50 mm displacement.

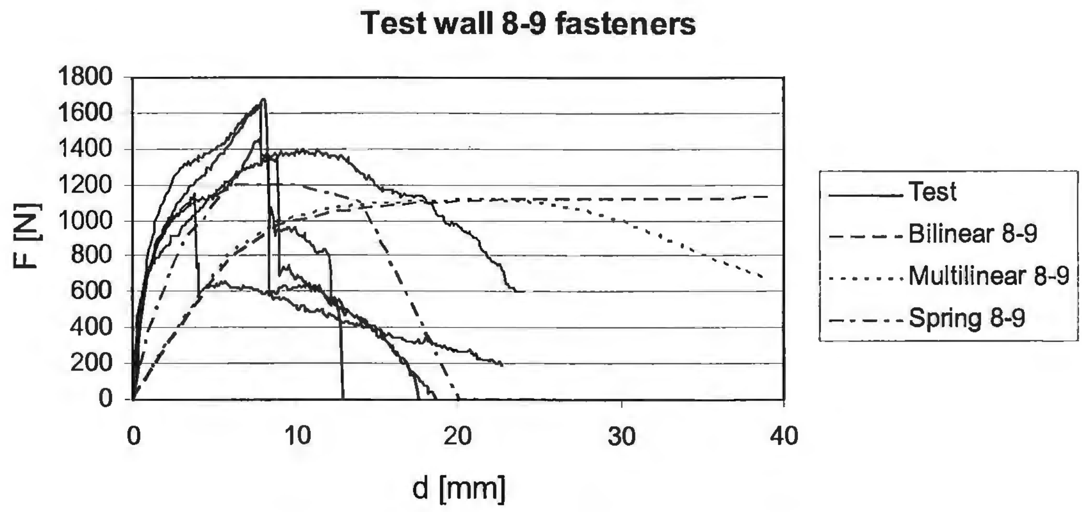

Figure 4.9: Force-displacement relationship of fasteners in tests and FE models.

As shown in Figure 4.9, the capacity of the modelled fasteners is lower than the capacities obtained from the fastener tests. It can be noted that also for plywood sheathed models the fasteners in the FE models have to be less stiff than the fasteners used in the tests in order for the modelled wall to obtain a stiffness similar to that of full scale test walls. As mentioned earlier, a possible cause is initial framing joint gaps, something that is not taken into account in the FE model.

4.4 Analyses

In the following, analyses of test walls 1-9 performed with the calibrated FE models are presented. The results are compared with the load carrying capacities obtained from experiments and the new analytical calculation model.

4.4.1 Test wall 1

Test wall 1, Figure 4.10 , is the wall described in chapter 4.3.1, after which the calibration of hardboard sheathed walls is performed. In this section, results from analyses with flexible framing and panels are presented together with experimental results and calibration curves in order to study the effects of the flexibility.

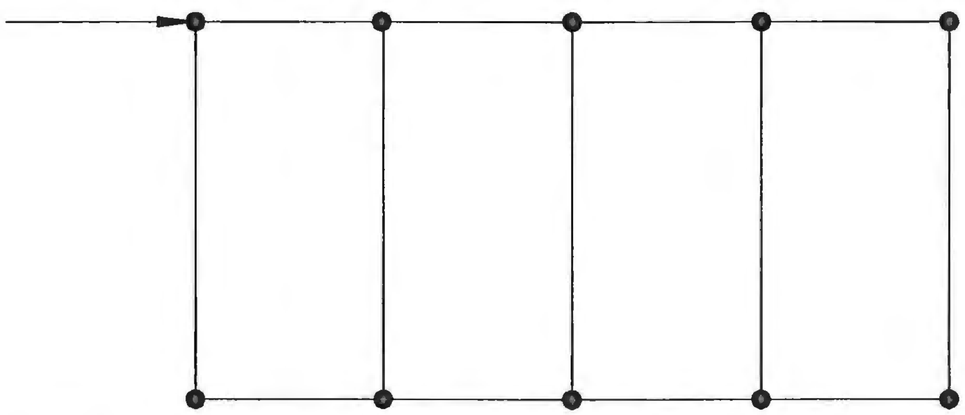

Figure 4.10: Loading and wall configuration for test wall 1.

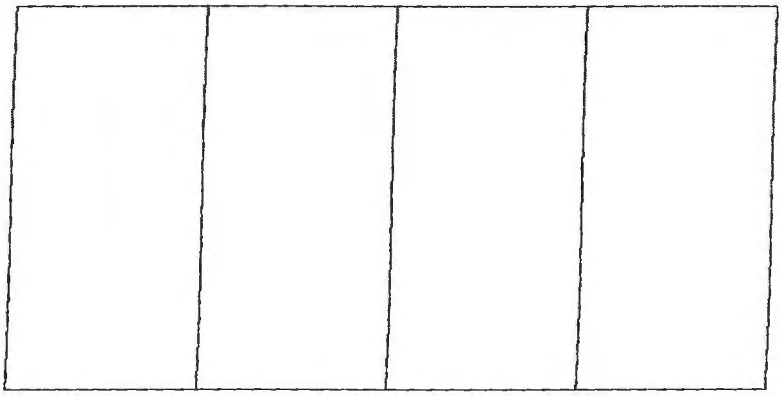

Figure 4.11: Deformation of framing according to FE model for test wall 1.

In the FE analyses, wall 1 is fully anchored with hinged framing joints. As can be observed in Figure 4.11, no uplift, i.e. separation of framing members, can occur.

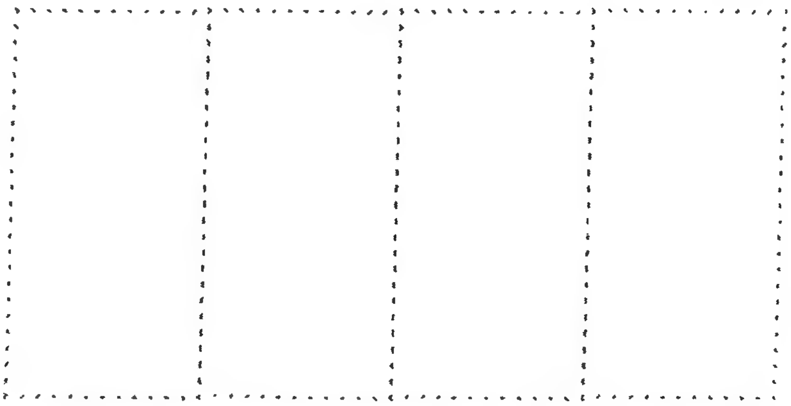

Figure 4.12: Plasticized fasteners according to FE model for test wall 1.

As shown in Figure 4.12, and as expected, all fasteners reach the plasticity limit at the maximum load carrying capacity, since the wall is exposed to a pure shear action.

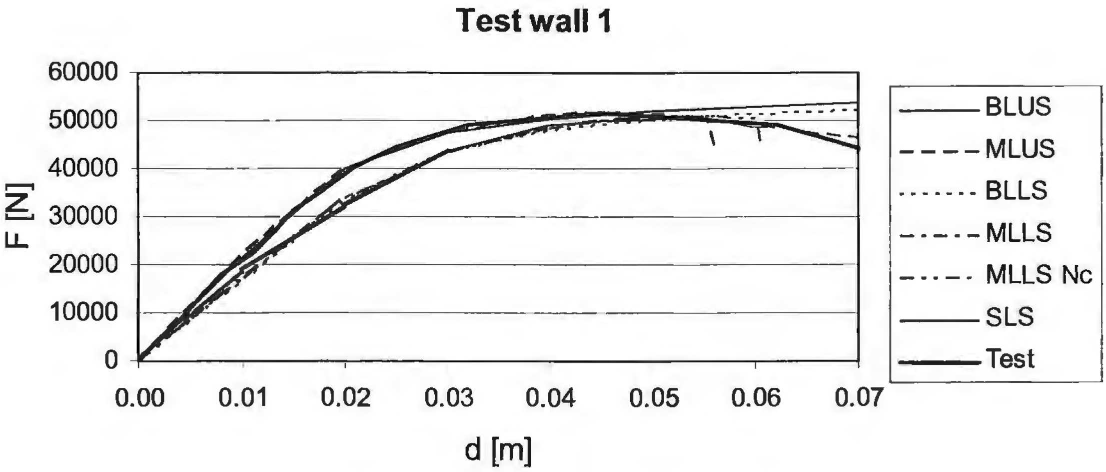

Figure 4.13: Force-displacement relationships obtained by FE analyses, and experimental test, for test wall 1.

BLUS, MLUS and SLS are the models that are calibrated after test wall 1. As can be seen in Figure 4.13, the models using flexible framing and sheathing are a bit less stiff. The difference between the maximum load carrying capacity of the models is quite small.

4.4.2 Test wall 2

Test wall 2, Figure 4.14, has a fully anchored bottom rail, no vertical load and no hold-downs. Walls with this kind of configuration ought to be the most complicated to model accurately by FE or analytical models of the 9 walls analysed.

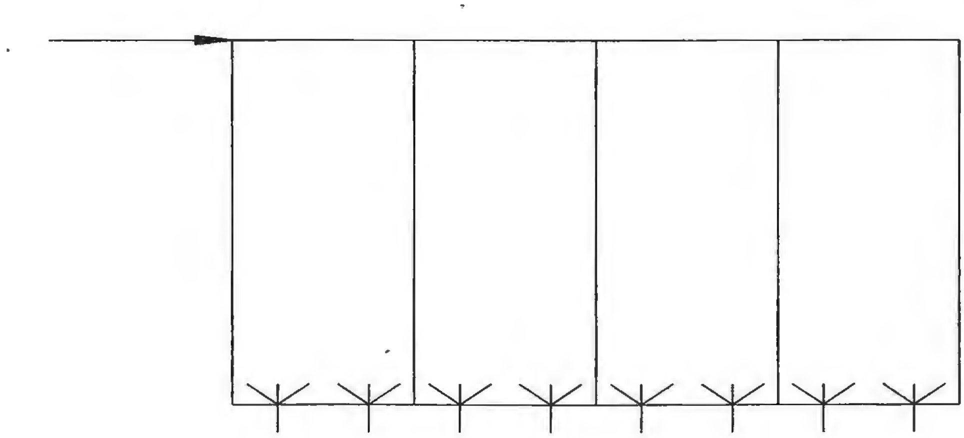

Figure 4.14: Loading and wall configuration for test wall 2.

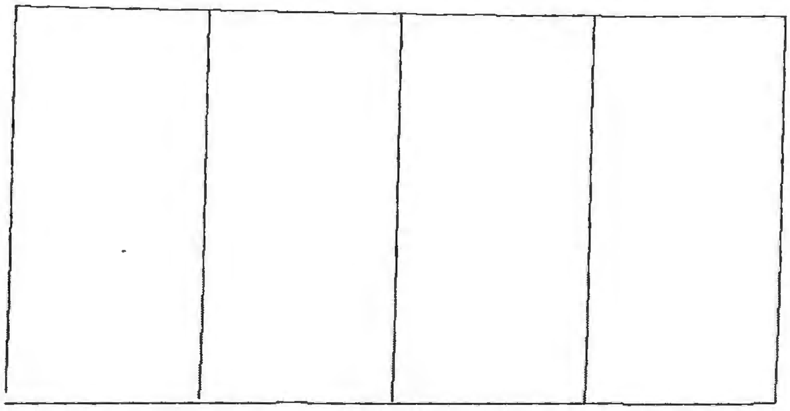

Figure 4.15: Deformation of framing according to FE model for test wall 2.

It can be seen in Figure 4.15 that the uplift is quite significant in this wall compared with wall 1. Not only the leading stud is separating from the bottom rail, but also the second and third stud. This is, of course, due to the lack of anchorage and vertical load. The consequence is a disturbed shear action of the wall.

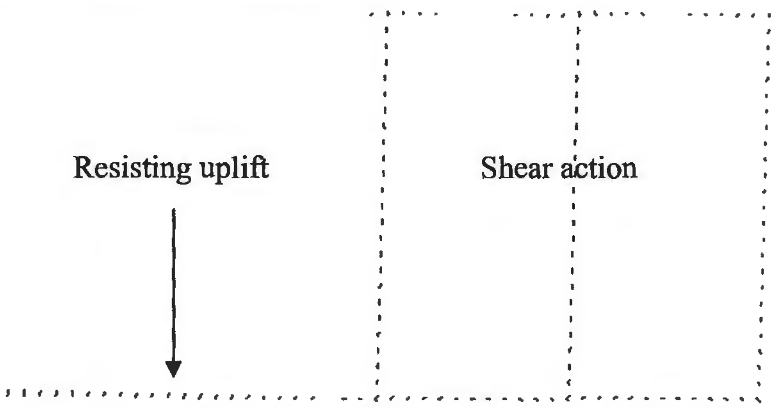

Figure 4.16: Plasticized fasteners according to FE model for test wall 2.

As can be observed in Figure 4.16, fasteners in the left part of the wall work as replacement for the omitted anchorage connection in a manner similar to what is assumed when using the analytical method, see Figure 2.5. The fasteners in the right part of the wall are exposed to a shear action, a behaviour that also corresponds to the force distribution in the analytical method.

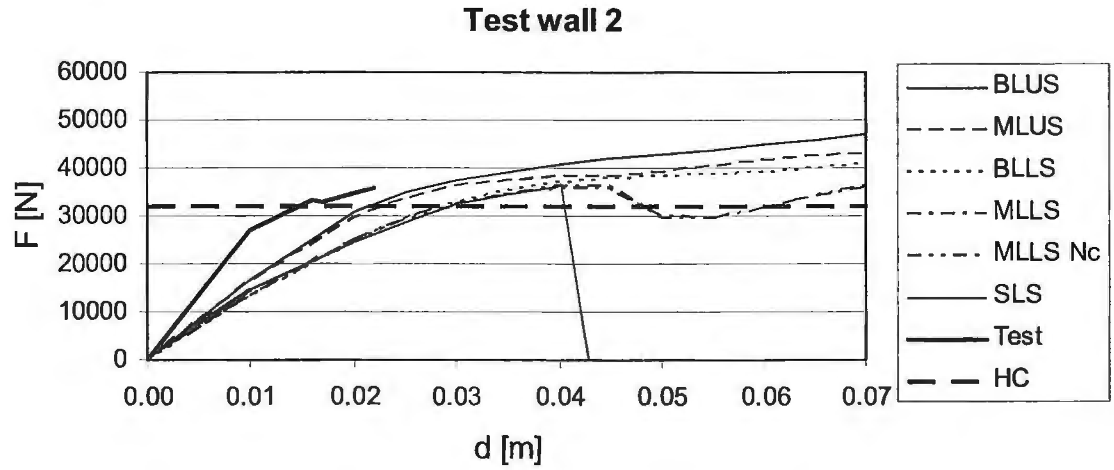

Figure 4.17: Force-displacement relationships obtained by FE analyses and experimental test, and maximum load carrying capacity obtained by analytical model, for test wall 2.

As shown in Figure 4.17, the analytical method HC and the MLLS model seem to correspond best to the maximum capacity of the test wall. Of the FE models, the MLLS and SLS models show the most realistic behaviour, at least until the horizontal displacement of the wall exceeds 40 mm. BLLS and BLUS do not work very well for this test wall. The difference between MLLS and MLUS is probably a result of the differences in framing and panel stiffness, an effect that is most pronounced after 40 mm. SLS seems to work quite well in spite of the limitations stated in chapter 3.1. The difference between MLLS and MLLS Nc, i.e. with or without the effects of the contact between adjacent sheets, is hardly noticeable. It can be noticed that the FE models are less stiff than the experimental wall. This phenomenon can be observed also for the rest of the test walls 2 – 7 and is therefore assumed to be a result of the calibration, implying that the test data for test wall 1 might be questionable, see section 5.1 Discussion.

4.4.3 Test wall 3

Test wall 3 has a fully anchored bottom rail, no framing joints and no vertical load, see Figure 4.18. The only difference between this wall and test wall 2 is the framing joints, which are present in test wall 2 and omitted in test wall 3.

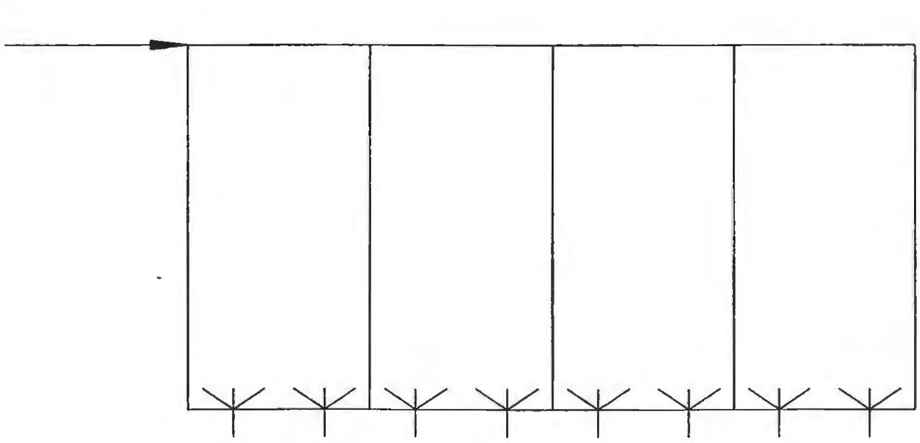

Figure 4.18: Loading and wall configuration for test wall 3.

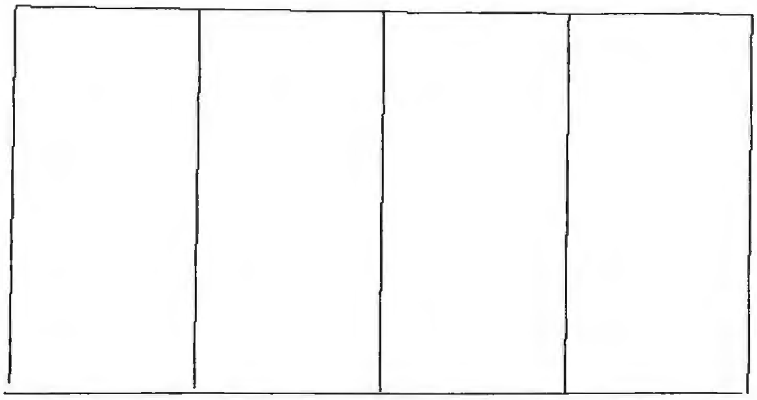

Figure 4.19: Deformation of framing according to FE model for test wall 3.

In Figure 4.19 a horizontal displacement of the studs, due to the lack of framing joints, can be observed. This effect decreases the load carrying capacity with about 10% in the experimental test compared to wall 2. A decrease of the same magnitude can be seen in the FE analyses, except for the bilinear fastener models, BLUS and BLLS. The uplift of the two most left studs of test wall 2, see Figure 4.15, of course, also occurs for test wall 3.

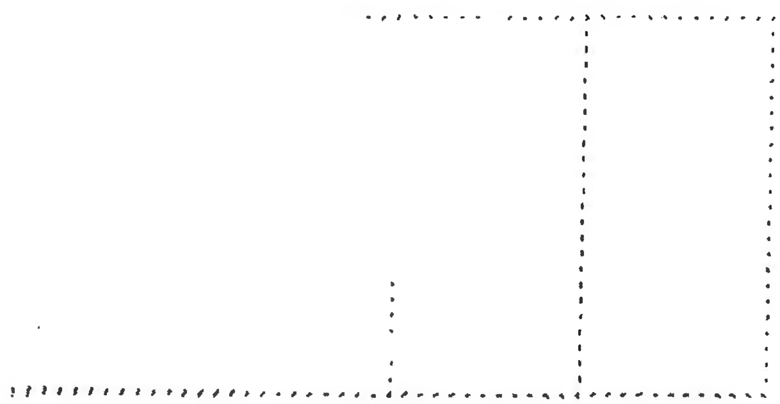

Figure 4.20: Plasticized fasteners according to FE model for test wall 3.

The fastener stresses, Figure 4.20, are rather similar to the ones in wall 2, Figure 4.16. The difference is that a number of fasteners located to the stud in the centre of the wall carry less load, which results in a slightly decreased load carrying capacity of the wall.

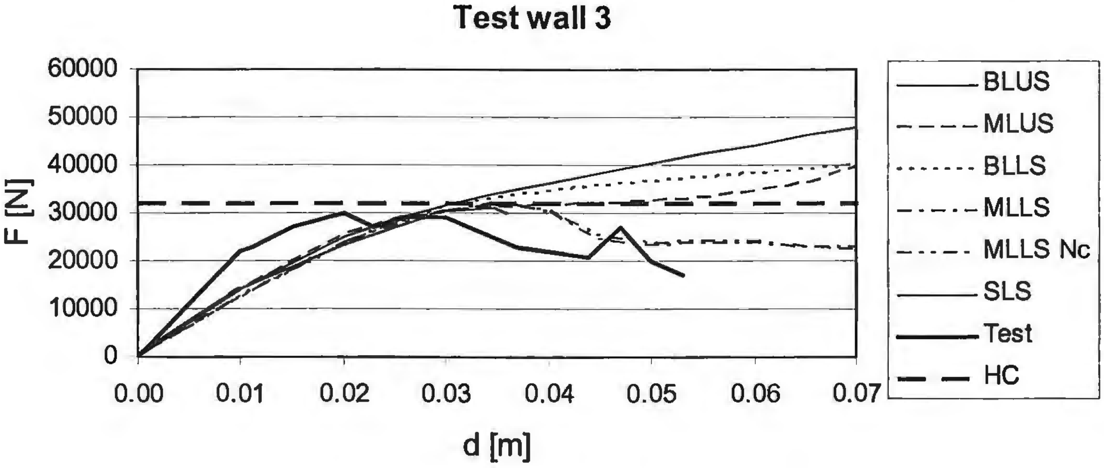

Figure 4.21: Force-displacement relationships obtained by FE analyses and experimental test, and maximum load carrying capacity obtained by analytical model, for test wall 3.

As can be seen in Figure 4.21, the MLLS and SLS models show the most realistic behaviour. HC does not take different framing joint conditions into account, why it gives the same result for test wall 2 and test wall 3. The greater overall stiffness of the models using rigid framing and panels compared to the other models, that can be observed for the other test walls, can hardly be noticed at all for test wall 3. Without framing joints, the stiffness of framing and sheathing, affects the behaviour of the model less than the case with framing joints. The maximum horizontal load of the multi-linear models occurs at a smaller displacement for this test wall compared with test wall 2. The slope of the force-displacement curve of the bilinear models also changes at the same displacement. Due to the fact that this occurs at an earlier stage than in the case of test wall 2, allows the horizontal load at a displacement of 70 mm to be of approximately of the same magnitude for both test wall 2 and 3, for the bilinear models. The same behaviour can be observed when studying the results of the other test wall analyses.

4.4.4 Test wall 4

Test wall 4 has a fully anchored bottom rail and a vertical load of 1.29 kN applied at each stud, as shown in Figure 4.22, which will counteract the uplift forces caused by the horizontal load.

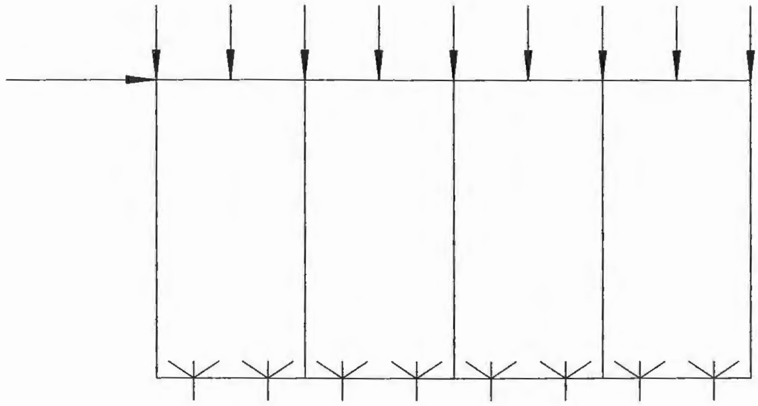

Figure 4.22: Loading and wall configuration for test wall 4.

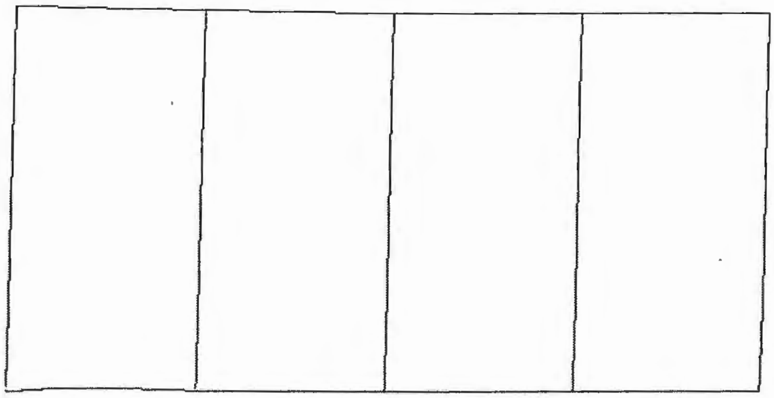

Figure 4.23: Deformation of framing according to FE model for test wall 4.

As shown in Figure 4.23, the uplift of the left part of the wall is not fully prevented by the vertical load, although it is decreased compared with the walls without vertical load.

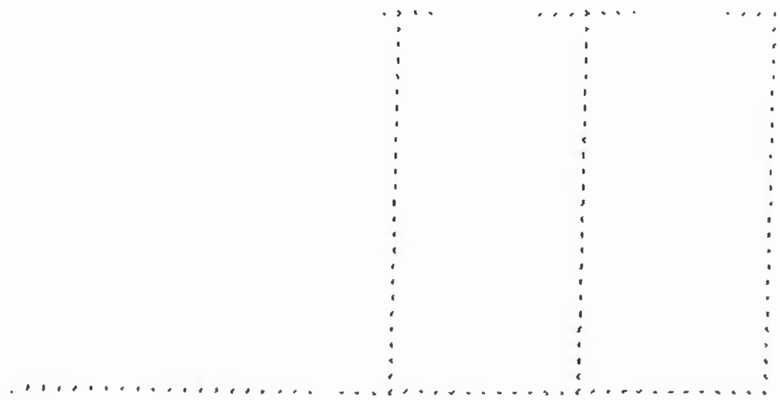

Figure 4.24: Plasticized fasteners according to FE model for test wall 4.

As can be observed in Figure 4.24, the uplift is still mainly prevented by the fasteners in the left part of the wall, as in the case of no vertical load. The right part of the wall seems to be exposed to pure shear action also for this load case.

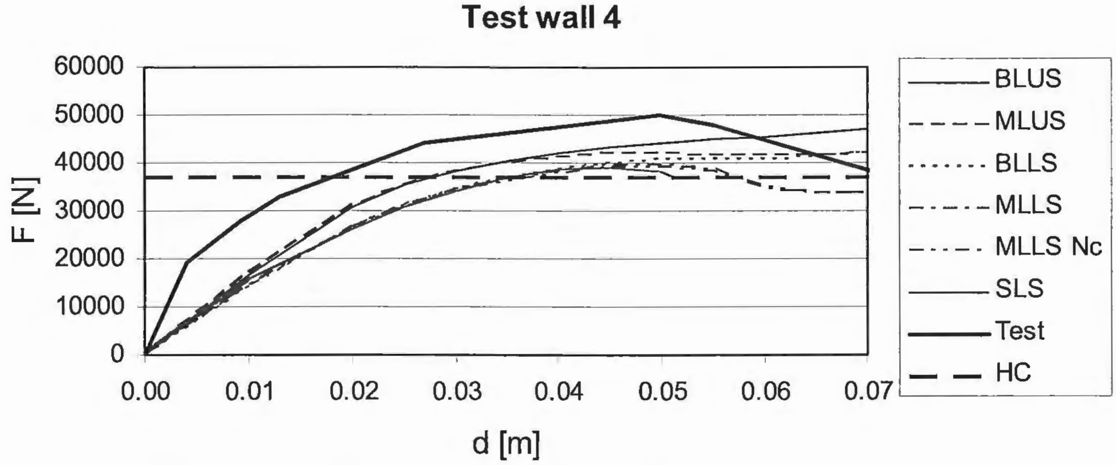

Figure 4.25: Force-displacement relationships obtained by FE analyses and experimental test, and maximum load carrying capacity obtained by analytical model, for test wall 4.

However, the vertical load drastically increases the load carrying capacity of the experimental wall, see Figure 4.25. This is something that the FE models do not really reflect. The analytical method is somewhat more accurate in relative terms. In absolute capacity, however, the analytical model deviates significantly from the experimental result. In this respect, BLUS and BLLS give the best results. This agrees with the assumption that bilinear models ought to be more and more accurate the closer the analysed walls are to full anchoring.

4.4.5 Test wall 5

Test wall 5 has a fully anchored bottom rail and a vertical load of 3.23 kN applied at each stud, see Figure 4.26. The test wall is almost similar to test wall 4, but with an increased vertical load.

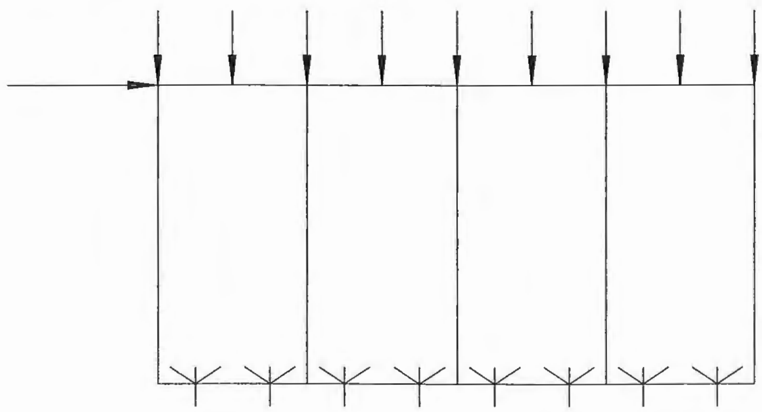

Figure 4.26: Loading and wall configuration for test wall 5.

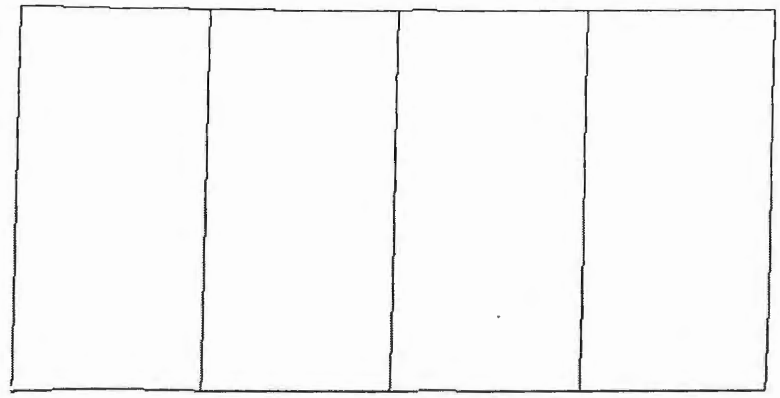

Figure 4.27: Deformation of framing according to FE model for test wall 5.

The increased vertical load results in decreased uplift of the left part of the wall. This can be observed by comparing Figure 4.27 and Figure 4.23.

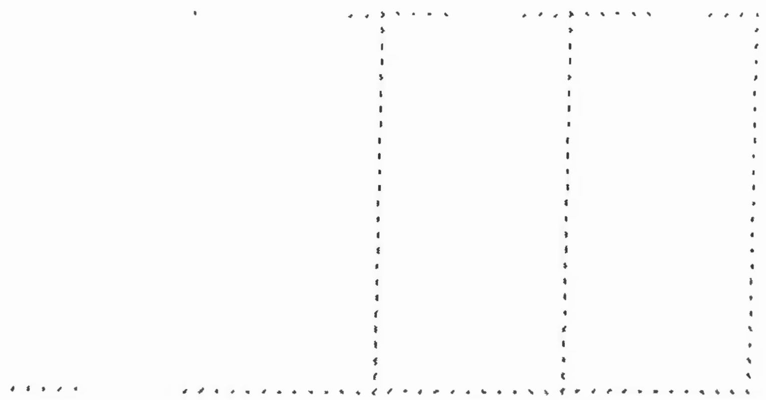

Figure 4.28: Plasticized fasteners according to FE model for test wall 5.

As can be observed in Figure 4.28, the increased vertical load consequently also decreases the vertical load on the fasteners in the left part of the wall.

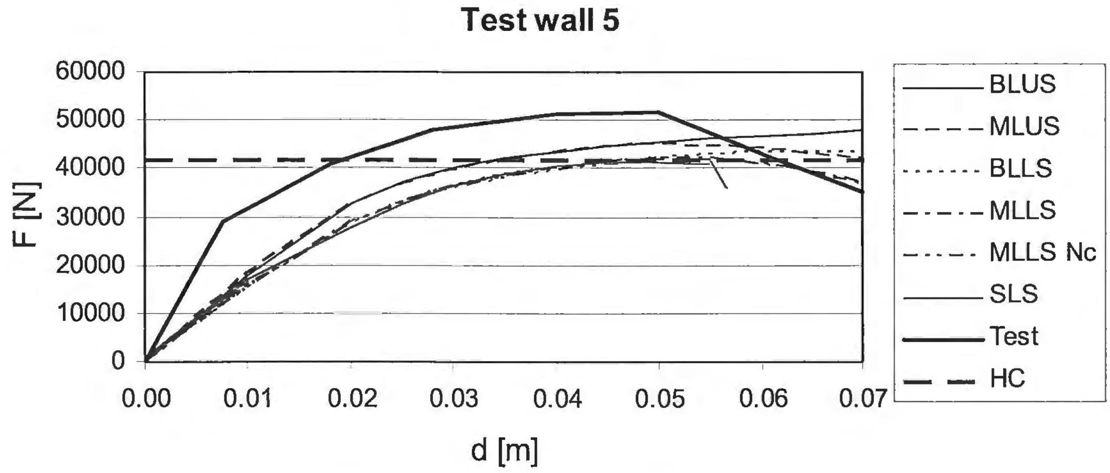

Figure 4.29: Force-displacement relationships obtained by FE analyses and experimental test, and maximum load carrying capacity obtained by analytical model, for test wall 5.

The increased vertical load leads to a somewhat increased load carrying capacity in both experimental test and analyses. Among the models, the increase is largest for the analytical method. The bilinear finite element models still gives the best accuracy, see Figure 4.29. However, it can be noted that the FE models and analytical method give very similar results. Since all models are calibrated after a fully anchored wall, it is of course reasonable that they will agree better for wall configurations close to that condition.

4.4.6 Test wall 6

Test wall 6 has a non-anchored bottom rail and a vertical load of 6.46 kN applied at each stud, as shown in Figure 4.30, which is twice the vertical load of test wall 5. The influence of the non-anchored bottom rail can be seen clearly in Figure 4.31, where the bottom rail is lifted from the substrate at the left wall end.

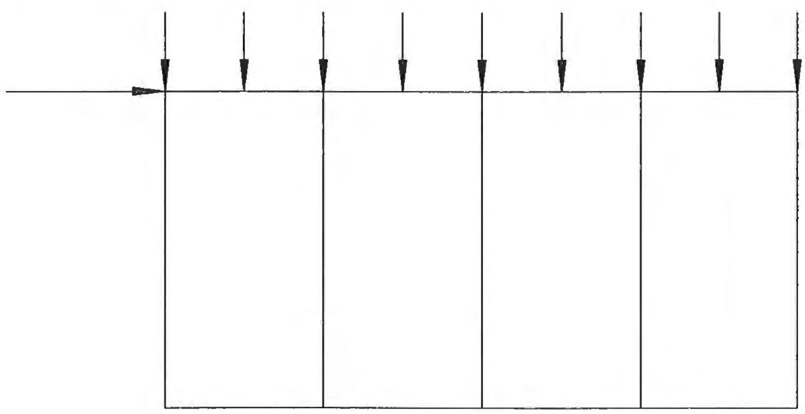

Figure 4.30: Loading and wall configuration for test wall 6.

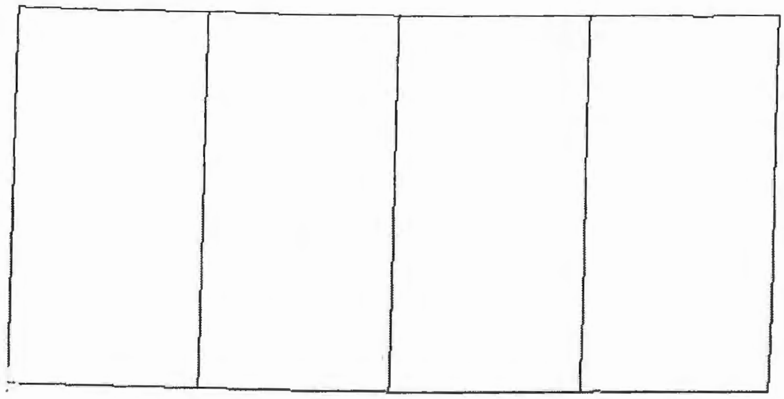

Figure 4.31: Deformation of framing according to FE model for test wall 6.

It can also be noted in Figure 4.32 that the hold-down action in the bottom rail fasteners is eliminated due to the release of the bottom rail. The shear action of the wall is still concentrated to the right wall part since the uplift is not completely prevented by the vertical force.

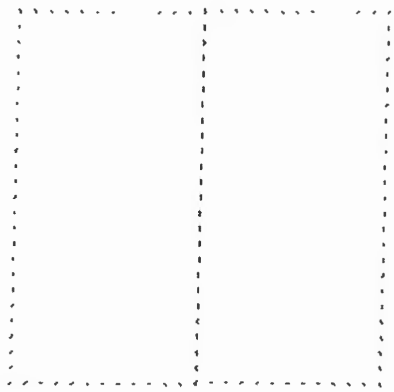

Figure 4.32: Plasticized fasteners according to FE model for test wall 6.

Consequently, the load carrying capacity is approximately the same for test wall 4 and 6, even though the vertical load is five times the vertical load of test wall 4, as a result of the difference in anchorage conditions.

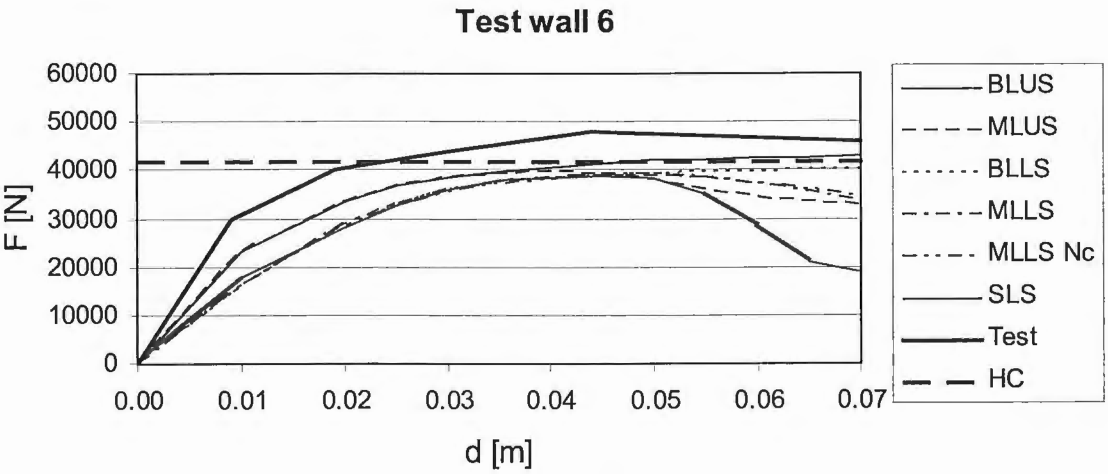

Figure 4.33: Force-displacement relationships obtained by FE analyses and experimental test, and maximum load carrying capacity obtained by analytical model, for test wall 6.

HC gives a better result for this test wall than those with fully anchored bottom rail and vertical load. BLUS, however, still gives the best result, as can be observed in Figure 4.33. The FE analyses all give rather similar results for this wall.

4.4.7 Test wall 7

Test wall 7 has a fully anchored bottom rail and a vertical load of 12.9 kN applied on the leading stud, as shown in Figure 4.34. A vertical load applied on the leading stud will, if it is large enough, give the wall a behaviour similar to that of a wall with a fully anchored leading stud. This is the case for wall 7, for which the capacity is quite close to the one of wall 1. It can also be seen in Figure 4.35 that the uplift is completely eliminated at the leading stud.

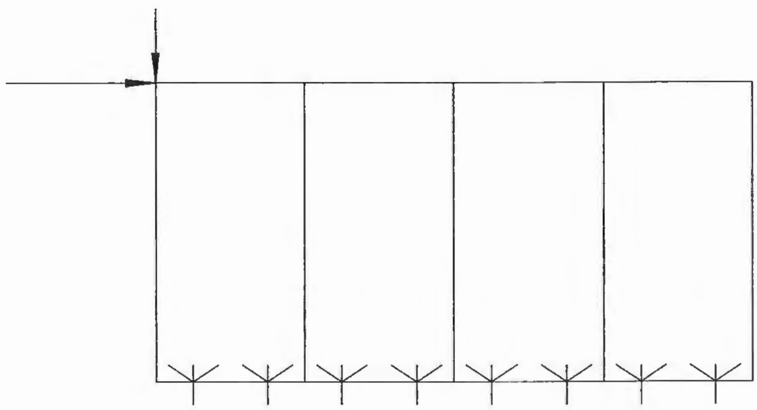

Figure 4.34: Loading and wall configuration for test wall 7.

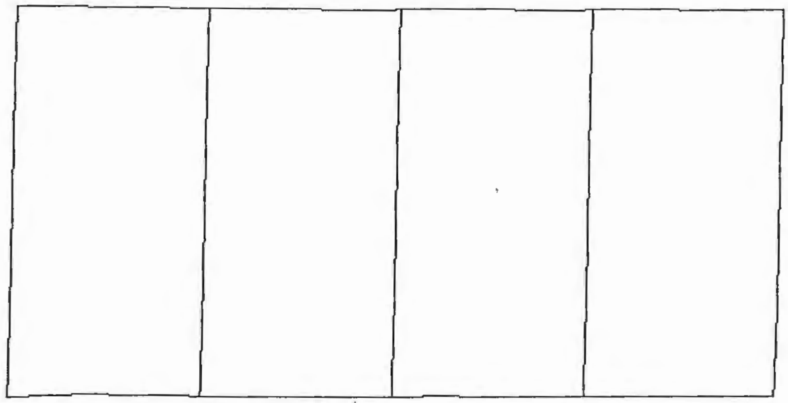

Figure 4.35: Deformation of framing according to FE model for test wall 7.

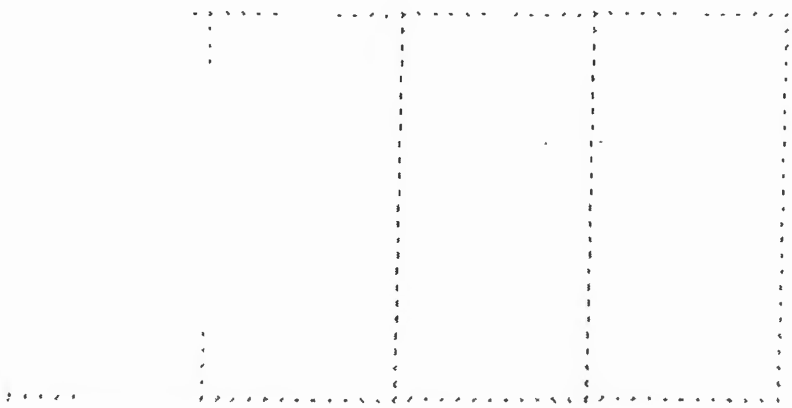

Figure 4.36: Plasticized fasteners according to FE model for test wall 7.

The wall is exposed to almost pure shear action, which can be seen in Figure 4.36.

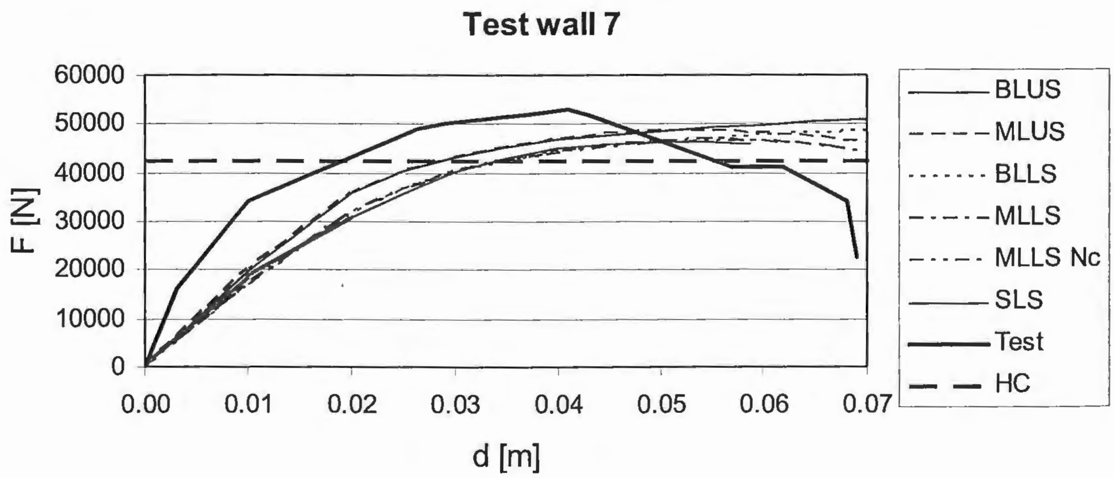

Figure 4.37: Force-displacement relationships obtained by FE analyses and experimental test, and maximum load carrying capacity obtained by analytical model, for test wall 7.

As a result of the significant vertical load, test wall 7 is the hardboard sheathed wall that according to the models and experiments, has the highest load carrying capacity, except for wall 1, see Figure 4.37. Since this wall is a wall rather similar to test wall 1, against which the FE models were calibrated, all the FE models are behaving in almost the same manner, but BLUS gives the best result. HC does not work as well as the FE models for this test wall.

4.4.8 Test wall 8

For the plywood sheathed walls, analyses have only been performed using flexible framing and sheathing. This is due to the fact that they are to be compared to analyses performed by Andreasson (2000), and therefore the same material properties are used.

Test wall 8, Figure 4.38, is the wall after which the fasteners for plywood sheathed walls are calibrated, described in chapter 4.3.2.

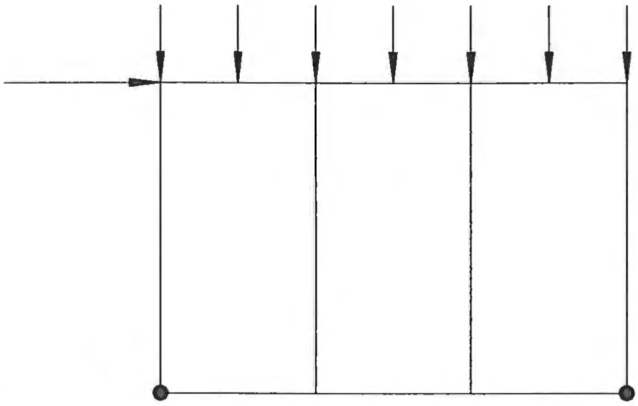

Figure 4.38: Loading and wall configuration for test wall 8.

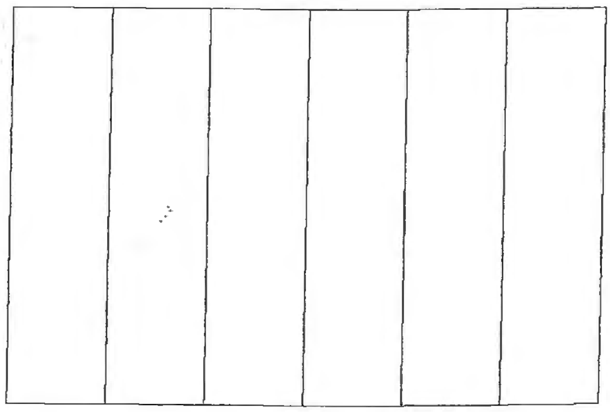

Figure 4.39: Deformation of framing according to FE model for test wall 8.

The deformation of the framing can be seen in Figure 4.39. The wall has flexible hold-downs at the wall ends and vertical load along the top rail, which to a large extent prevent uplift.

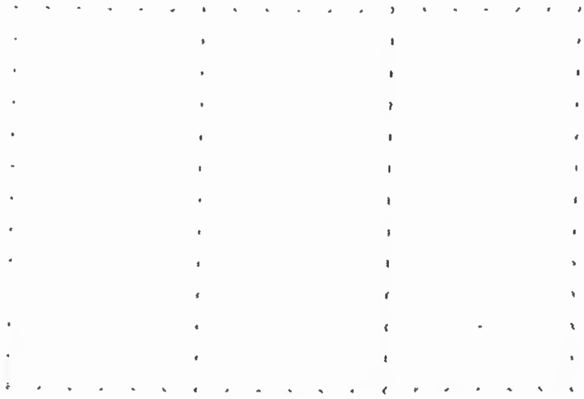

Figure 4.40: Plasticized fasteners according to FE model for test wall 8.

As can be seen in Figure 4.40, and as can be expected in the case of a fully anchored wall, almost every fastener has been plasticized.

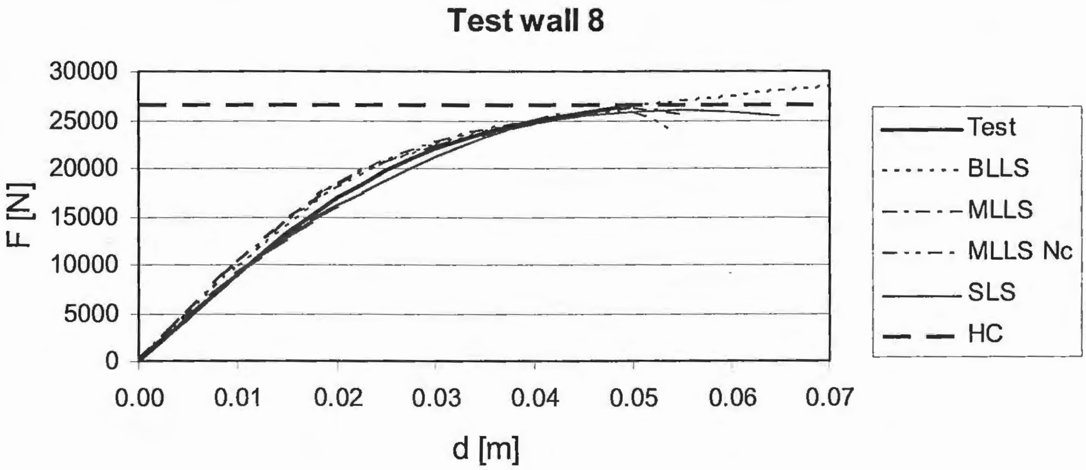

Figure 4.41: Force-displacement relationships obtained by FE analyses and experimental test, and maximum load carrying capacity obtained by analytical model, for test wall 8.

All models, in Figure 4.41, have been calibrated against test wall 8, which explains the agreement between the results.

4.4.9 Test wall 9

Test wall 9 contains an opening and is fully anchored to the substrate with hold-downs at wall ends and at the opening, as can be seen in Figure 4.42. The wall is not subjected to any vertical load. The behaviour of a wall with openings is much affected by brittle failure modes, more than in the case of a wall without openings. This will probably make the prediction of the behaviour of such a wall less accurate.

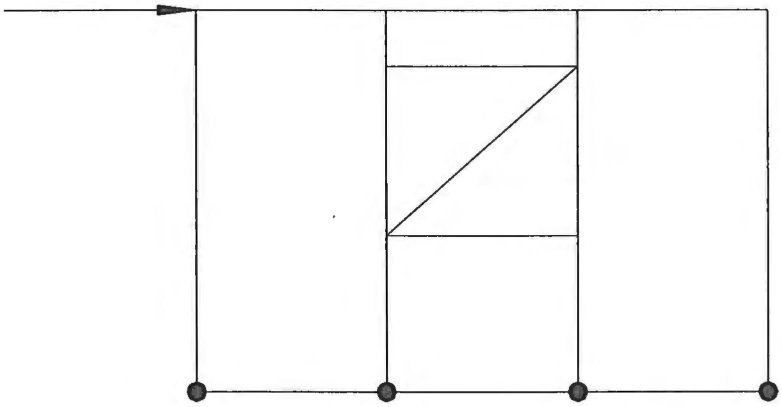

Figure 4.42: Loading and wall configuration for test wall 9.

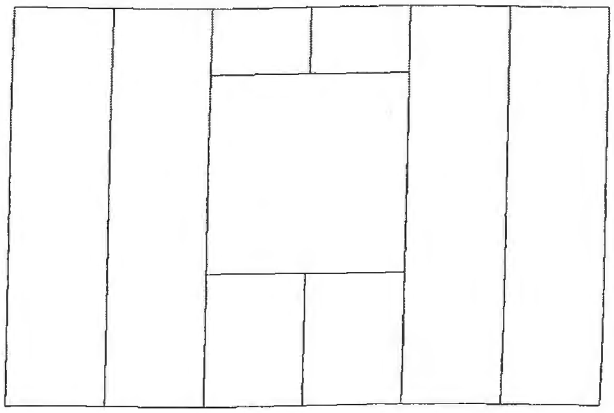

Figure 4.43: Deformation of framing according to FE model for test wall 9.

No uplift etc can of course be observed in Figure 4.43.

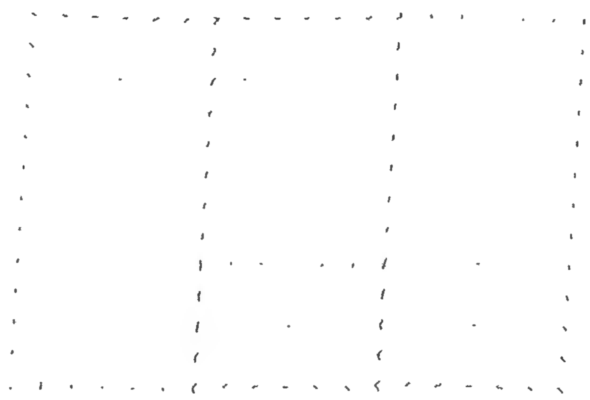

Figure 4.44: Plasticized fasteners according to FE model for test wall 9.

As can be seen in Figure 4.44, not many of the centre stud fasteners are plasticized. The fasteners at the window rails also carry less load than the other perimeter fasteners.

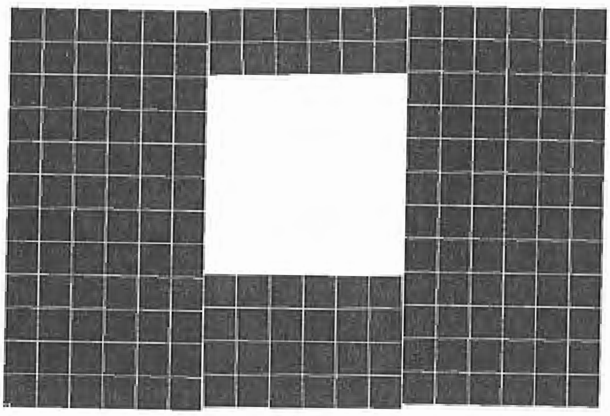

Figure 4.45: Deformation of panels according to FE model for test wall 9.

The rotation of the panels can be seen in Figure 4.45.

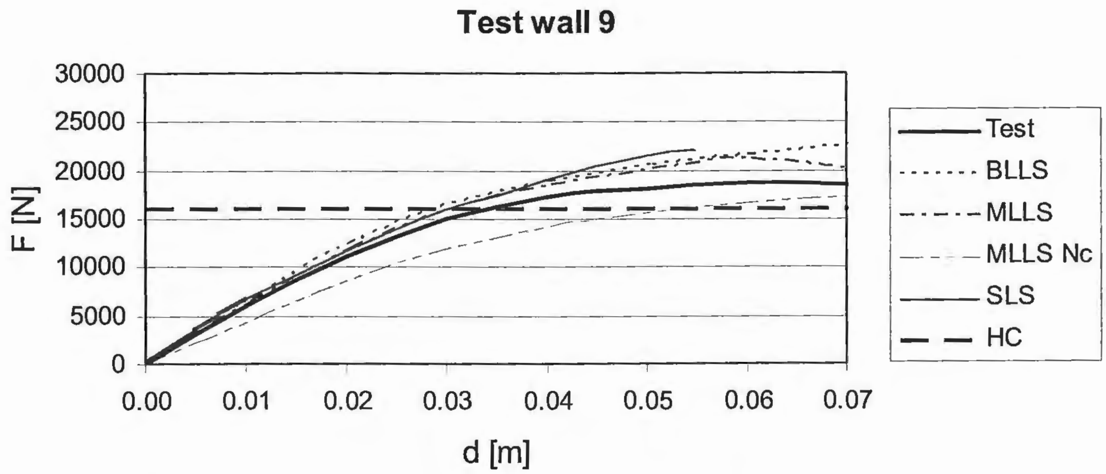

Figure 4.46: Force-displacement relationships obtained by FE analyses and experimental test, and maximum load carrying capacity obtained by analytical model, for test wall 9.

For this test wall the influence of contact between adjacent panels (see MLLS respective MLLS Nc) is quite noticeable, which it is not the case for the previous test walls without opening. The load carrying capacity of the FE models with contact elements between adjacent sheets, is greater than the one obtained from experiments, while the load carrying capacity obtained from the analytical method is smaller, as can be seen in Figure 4.46. However, the results are of the same accuracy as for the other wall configurations. It can be noted that the new FE model, MLLS, gives somewhat better results than the original de-coupled spring model, SLS. The difference is not as large as could be expected, though. The result given by the analytical method is also remarkably good for a wall of this complexity.

4.5 Results

In the tables, the results of comparisons between load carrying capacities obtained with the new analytical method, the FE models and experimental tests are presented.

Table 4.6: Calculated and measured load carrying capacities in Newton.

Test wall	Test	Hc	BLUS	MLUS	BLLS	MLLS	MLLS Nc	SLS
1	51700				52069	50724	50773	
2	33200	31900	46903	43051	40816	36207	36100	36214
3	29400	31900	47745	39404	40144	32246	31870	31298
4	50100	37000	46981	42075	41968	39662	39292	39251
5	52500	41600	47832	44906	43652	42141	41775	41481
6	48200	42000	42945	39807	40111	39266	38983	38780
7	53100	42500	50800	48578	48357	46740	46441	46586
8	26600	26494					25715	26176
9	18600	16111			22555	21245	17489	22258

As can be observed in Table 4.6, the FE models seem to react in the same way as the experimental walls to changes of load and anchorage conditions, with the exception of test wall 1. Changes that increase, alternatively decrease, the load carrying capacity of the experimental wall, have the same influence on the FE models. The analytical model does not show the same agreement concerning changes in load and anchorage conditions.

Furthermore, it can be seen in the graphs that the different FE models tested all show a similar behaviour until a certain deformation is reached. The maximum load carrying capacity of most models also occurs at this stage of deformation. If the deformation is further increased, the models using a bilinear fastener material model show a deviant behaviour by still allowing the wall to carry more and more load. This makes the bilinear models least capable of describing the structural behaviour of a shear wall of the models tested.

Surprisingly enough, the de-coupled spring model in the original FE model gives almost as good results as the best of the further developed models with beam elements representing the fasteners. This indicates that there are other important phenomena in connection to the fastener representation that must be implemented in order to make any difference between the simplest and more advanced models. One important feature might be direction dependent fastener properties.

Of the two material properties used, rigid respective flexible framing and sheathing, the more flexible variant is to prefer. An increased stiffness of sheathing and framing not only makes the model capable of carrying more load, but it also makes the model capable of handling large deformation in a manner a real wall would not..

The usage of contact elements to simulate the effects of contact between adjacent sheets does not affect the behaviour of any of the models significantly when using flexible framing and sheathing, in the case of walls without openings. The difference is, however, quite large for a wall with opening.

Table 4.7: Relative comparison between load carrying capacities from FE analyses respective experimental tests and the new analytical method.

Test wall	Test/Hc	BLUS/ Hc	MLUS/ Hc	BLLS/ Hc	MLLS/ Hc	MLLS Nc/Hc	SLS/Hc
1							
2	1.04	1.47	1.35	1.28	1.14	1.13	1.14
3	0.92	1.50	1.24	1.26	1.01	1.00	0.98
4	1.35	1.27	1.14	1.13	1.07	1.06	1.06
5	1.26	1.15	1.08	1.05	1.01	1.00	1.00
6	1.15	1.02	0.95	0.96	0.93	0.93	0.92
7	1.25	1.20	1.14	1.14	1.10	1.09	1.10
8	1.00					0.97	0.99
9	1.15			1.40	1.32	1.09	1.38

Table 4.8: Relative comparison between load carrying capacities from FE analyses respective the new analytical method and experimental tests.

Test wall	Hc/Test	BLUS/Test	MLUS/ Test	BLLS/ Test	MLLS/ Test	MLLS Nc/Test	SLS/Test
1				1.01	0.98	0.98	
2	0.96	1.41	1.30	1.23	1.09	1.09	1.09
3	1.09	1.62	1.34	1.37	1.10	1.08	1.06
4	0.74	0.94	0.84	0.84	0.79	0.78	0.78
5	0.79	0.91	0.86	0.83	0.80	0.80	0.79
6	0.87	0.89	0.83	0.83	0.81	0.81	0.80
7	0.80	0.96	0.91	0.91	0.88	0.87	0.88
8	1.00					0.97	0.98
9	0.87			1.21	1.14	0.94	1.20

As can be seen in Table 4.7, and Table 4.8, the best FE model (MLLS) is least accurate for test walls 4, 5 and 6. The analytical method, on the contrary, seems to be least accurate for walls 4, 5 and 7.

Table 4.9: Difference between largest and smallest load carrying capacity ratio.

Max -Min	Hc/ Test	BLUS/ Test	MLUS/ Test	BLLS/ Test	MLLS/ Test	MLLS Nc/Test	SLS/Test
	0.35	0.73	0.51	0.53	0.35	0.30	0.41

Both the FE method and the analytical method seem to have quite the same accuracy. The ratio between the calculated and measured load carrying capacity ranges between 0.74 and 1.09 for the analytical method and between 0.79 and 1.14 for the FE model with multi-linear beam elements and flexible framing and panels, MLLS. The differences between the major and minor ratios are presented in Table 4.9.

Table 4.10: Influence of framing joints.

Test wall	Test	Hc	BLUS	MLUS	BLLS	MLLS	MLLS Nc	SLS
2/3	1.13	1.00	0.98	1.09	1.02	1.12	1.13	1.16

The effects of omitting the framing joints in the wall construction are taken into account when using the FE models, but not when using the analytical method. For the models using spring or multi-linear beam elements for fastener representation, the existence of framing joints does increase the load carrying capacity by approximately 10 to 15 %, compared to the case of no framing joints, see Table 4.10. This agrees very well with the experimental results.

In order to obtain a model with a behaviour similar to that of an experimental wall, the fasteners must be less stiff than the fastener stiffness obtained from small scale fastener tests, as illustrated in Figure 4.6, at least if all framing to sheathing joints are supposed to have the same characteristics as they have in these models.

To use flexible framing and panels together with multi-linear beam elements for fastener representation seems to be the best way of modelling a shear wall when using the finite element method.

5 Discussion and conclusions

The main objective of the study was to compare the accuracy of a new analytical method for partially anchored and vertically loaded shear walls with the accuracy of advanced FE analyses. Furthermore, the behaviour of FE models with different complexity of fastener representation was to be studied in order to get an understanding of the level of detail needed for such a model. These objectives have been reached. In the following, the validity of the results and the analyses performed will be discussed, and major conclusions will be stated.

5.1 Discussion

First of all, it is important to bear in mind that the reliability of the test data, used for calibration and comparisons, is questionable since only one experiment was performed on each wall type. This may have had effect on the calibration of the model and thereby also on the results of the analyses. Even if the wall after which the model is calibrated is representative, the other wall capacities might be incorrect, which will make the comparisons misleading. As can be noticed the experimental walls, test wall 2 - 7, are consistently stiffer than the FE models, which indicates that the experimental data used for calibration, test wall 1, might be misleading.

In the calibration of the model it was observed that the fastener must be less stiff than the stiffness obtained from small scale fastener tests in order to get a model with a behaviour similar to that of an experimental wall, as illustrated in Figure 4.6 and Figure 4.9. However, since test wall 2 - 7, were stiffer than the corresponding FE analyses, this might be due to some defects of test wall 1, after which the fastener models are calibrated. In order to investigate if that is the only reason for the deviation between the small scale tests and the calibrated fastener models, one of the models was calibrated after another test wall as well, see Figure 5.1.

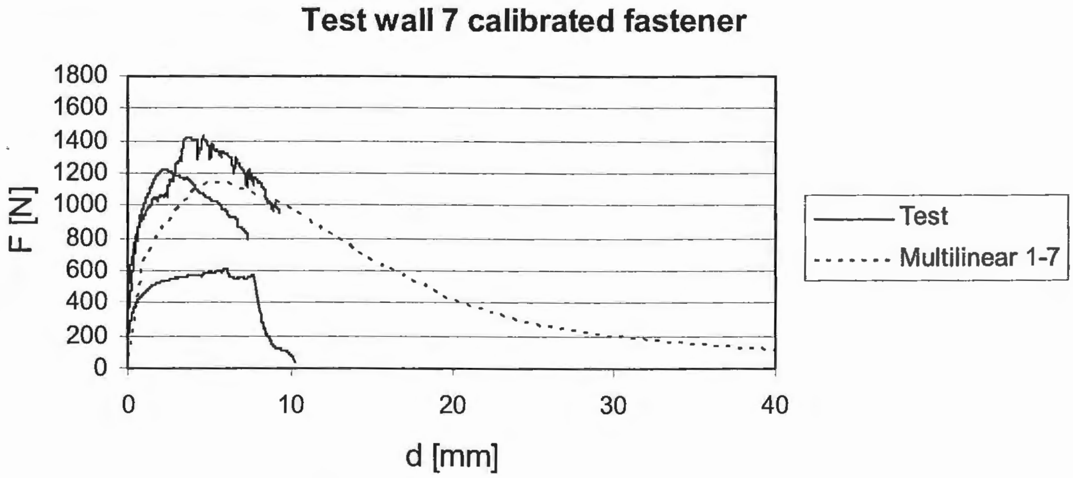

Figure 5.1: Force-displacement relationship of fasteners in tests and FE model.

Figure 5.1 shows the properties of a fastener model which was calibrated against test wall 7. It can be noticed that this fastener model shows a behaviour more similar to that of small scale fastener tests, compared to the fastener models calibrated against test wall 1, but it is still less stiff than a fastener should be according to the fastener tests.

This is probably a result of initial framing joint gaps. The impact of this phenomenon on the results is not known. A way of solving this discrepancy might be to use a fastener model with a stiffness obtained from small scale tests, but let a number of fasteners not take any load until they have been exposed to a certain deformation. The fasteners used in the models in this study all have the same force-displacement characteristics and in all directions (except the original de-coupled spring model, SLS). The use of a fastener representation with different characteristics in different directions, e.g. beam elements with non circular cross sections, might also make the model behave in a more realistic way. ANSYS, however, showed to be somewhat limited when it comes to material models and the possibility to use them in combination with certain elements.

5.2 Conclusions

The conclusions concerning different FE models are presented in Chapter 5.2.1, while conclusions concerning FE models in general and the analytical method are presented in Chapter 5.2.2.

5.2.1 Comparisons of FE models

The fasteners are the most crucial components of all the components modelled. The properties of the fastener element directly affect the overall performance of a wall.

The results of the analyses show that:

- The bilinear models are only useable in the case of a fully anchored wall or a wall behaving in a similar way as a result of vertical load.
- A model with flexible framing and panel elements seems to be preferable compared to a model with rigid elements. An increased panel and framing stiffness makes the model stiffer and capable of carrying more load, but it also makes the model capable of handling very large deformations in a manner that a real wall would not do.
- The use of beam elements instead of de-coupled spring elements representing the fasteners brought about only minor improvements on the model behaviour.
- The usage of contact elements to simulate the effects of contact between adjacent sheets does not affect the behaviour of the models significantly if it is a wall without openings that is analysed. The difference is less than 1%.
- The influence of contact elements between adjacent sheets is significant if it is a wall with openings that is analysed. The difference in load carrying capacity can be up to 20%.
- For the models using spring or multi-linear beam elements for fastener representation, the existence of framing joints increases the load carrying capacity by approximately 10%, compared to the case when the framing joints are omitted. This is well in accordance with the experimental results.

5.2.2 Comparison of methods

When comparing the results obtained by each model some general conclusions can be drawn:

- Both the analytical method and the most advanced FE model seem to be quite accurate.
- The analytical method is as accurate as the FE models.
- The ratios between calculated and experimental load carrying capacities for the analytical method vary between 0.74 - 1.09 and corresponding ratios for the best FE model (MLLS) vary between 0.79 - 1.14.
- The FE models are most accurate when they are used for analyses of walls that are close to fully anchored. The accuracy of the analytical model is not so clearly connected to any specific loading and anchorage conditions.
- It is not possible to take full advantage of the positive effects of vertical load, when using any of the methods tested. The experimental load carrying capacity is far more increased than the capacity obtained from any of the models.
- The changes of the load carrying capacity (in respect of positive or negative change) is almost identical between the experimental results and the most advanced FE model, while the relation is more arbitrary between the experimental results and the analytical model.

To conclude, it can be stated that the most accurate way of modelling a shear wall with FE models ought to be to use a realistic stiffness for framing and panel elements, and to use multi-linear beam elements as fastener elements. Furthermore, the use of beam elements instead of de-coupled spring elements as fastener representation in FE models gives no major improvement of the model accuracy. In order to develop a more accurate model this measure alone is not enough.

It can also be stated that the new analytical model gives results of the same accuracy as the best finite element model used in this study. The analytical model has proven to be quite accurate for analyses of different walls compared to experimental results, also for more complex wall configurations.

5.3 Further work

In order to get a more accurate FE model that can motivate the use of finite element analyses for this kind of design problems, it is important to make further investigations concerning some specific issues:

- The impact of a fastener model with different fastener properties in different directions (e.g. parallel and perpendicular to the sheathing edge).
- The influence of initial gaps between framing members and/or in the sheathing to framing joints.
- The conformity between tests, FE analyses and the new analytical model for more wall configurations, especially with openings and only partially anchored walls.

It is also of great interest to develop fastener elements with the possibility of brittle failure in order to make it possible to use fastener characteristics which are more like those in small scale fastener tests.

6 References

Andreasson S., (2000), Three-Dimensional Interaction in Stabilisation of Multi-Storey Timber Frame Building Systems, Licentiate Thesis, Division of Structural Engineering, Lund Institute of Technology, Lund University

Carling O. et al., (1992), Dimensionering av Träkonstruktioner (Design of timber structures), AB Svensk Byggtjänst, Solna, Sweden

Källsner B., Girhammar U. A. and Wu, L. (2001). A simplified plastic model for design of partially anchored wood framed shear walls. CIB/W18 Meeting, Venice, Italy, 22-24 August, 2001.

Wu L., Girhammar U. A. and Källsner B. (2002). Tests of Partially Anchored Wood Framed Shear Walls. Dept. of Applied Physics, Umeå University of Technology (not yet published).

Kohnke P., (1999), ANSYS Theory Reference Release 5.6

Källsner B., Lam F., (1995), Diaphragms and shear walls, STEP 3. Holzbauwerke, Grundlagen, Entwicklungen, Ergänzungen. Fachverlag Holz, Düsseldorf, pp. 15/1-15/19